

Narrow Bandgap Covalent Organic Frameworks with Strong Optical Response in the Visible and Infrared

Supporting Information

Li-Ming Yang*¹, Eric Ganz², Song Wang,³ Xiao-Jun Li,⁴ and Thomas Frauenheim¹

¹Bremen Center for Computational Materials Science, University of Bremen, Am Falturm 1, 28359, Bremen, Germany; ²Department of Physics, University of Minnesota, 116 Church St., SE, Minneapolis, Minnesota 55416, USA; ³State Key Laboratory of Theoretical and Computational Chemistry, Institute of Theoretical Chemistry, Jilin University, Changchun 130023, People's Republic of China. ⁴School of Chemistry and Chemical Engineering, Xi'an University, Xi'an 710065, Shaanxi Province, P.R. China (email: lmyang.uio@gmail.com)

Page 2, **Table S1**. The optimized equilibrium lattice constants, bulk moduli, and its pressure derivatives.
Page 3, **Fig. S1**. The calculated electronic band structure of (C, Si).
Page 4, **Fig. S2**. The calculated electronic band structure of (C, Ge).
Page 5, **Fig. S3**. The calculated electronic band structure of (C, Sn).
Page 6, **Fig. S4**. The calculated electronic band structure of (C, Pb).
Page 7, **Fig. S5**. The calculated electronic band structure of (Si, C).
Page 8, **Fig. S6**. The calculated electronic band structure of (Si, Si).
Page 9, **Fig. S7**. The calculated electronic band structure of (Si, Ge).
Page 10, **Fig. S8**. The calculated electronic band structure of (Si, Sn).
Page 11, **Fig. S9**. The calculated electronic band structure of (Si, Pb).
Page 12, **Table S2**. The estimated band gaps and corresponding wavelengths of absorption lights for the whole (X, Y) series.
Page 13, **Fig. S10**. The calculated TDOS and PDOS for (C, Si)
Page 14, **Fig. S11**. The calculated TDOS and PDOS for (C, Ge)
Page 15, **Fig. S12**. The calculated TDOS and PDOS for (C, Sn)
Page 16, **Fig. S13**. The calculated TDOS and PDOS for (C, Pb)
Page 17, **Fig. S14**. The calculated TDOS and PDOS for (Si, C)
Page 18, **Fig. S15**. The calculated TDOS and PDOS for (Si, Si)
Page 19, **Fig. S16**. The calculated TDOS and PDOS for (Si, Ge)
Page 20, **Fig. S17**. The calculated TDOS and PDOS for (Si, Sn)
Page 21, **Fig. S18**. The calculated TDOS and PDOS for (Si, Pb)
Page 22, **Fig. S19**. The calculated charge density, charge transfer, and ELF plots for (C, Si)
Page 23, **Fig. S20**. The calculated charge density, charge transfer, and ELF plots for (C, Ge)
Page 24, **Fig. S21**. The calculated charge density, charge transfer, and ELF plots for (C, Sn)
Page 25, **Fig. S22**. The calculated charge density, charge transfer, and ELF plots for (C, Pb)
Page 26, **Fig. S23**. The calculated charge density, charge transfer, and ELF plots for (Si, C)
Page 27, **Fig. S24**. The calculated charge density, charge transfer, and ELF plots for (Si, Si)
Page 28, **Fig. S25**. The calculated charge density, charge transfer, and ELF plots for (Si, Ge)
Page 29, **Fig. S26**. The calculated charge density, charge transfer, and ELF plots for (Si, Sn)
Page 30, **Fig. S27**. The calculated charge density, charge transfer, and ELF plots for (Si, Pb)
Page 31, **Table S3**. The calculated formation enthalpies for the whole (X, Y) series.
Pages 32-41, **Figs. S28-S37**. The calculated optical properties for each material.
Page 32, **Fig. S28**. The calculated optical properties for (C, C)
Page 33, **Fig. S29**. The calculated optical properties for (C, Si)
Page 34, **Fig. S30**. The calculated optical properties for (C, Ge)
Page 35, **Fig. S31**. The calculated optical properties for (C, Sn)
Page 36, **Fig. S32**. The calculated optical properties for (C, Pb)
Page 37, **Fig. S33**. The calculated optical properties for (Si, C)
Page 38, **Fig. S34**. The calculated optical properties for (Si, Si)
Page 39, **Fig. S35**. The calculated optical properties for (Si, Ge)
Page 40, **Fig. S36**. The calculated optical properties for (Si, Sn)
Page 41, **Fig. S37**. The calculated optical properties for (Si, Pb)
Page 42, **Table S4**. Optical constants at infinite wavelength or zero energy: $\epsilon_1(0)$, $R(0)$, $n(0)$, and the maximum peaks of imaginary part of dielectric function $\epsilon_2(\omega)$, extinction coefficient $k(\omega)$, the real part of optical conductivity $Re(\sigma)$, electron energy-loss function $L(\omega)$, absorption coefficient $\alpha(\omega)$ for the whole (X,Y) series as well as that of MOF-5 for a comparison.
Page 43, **Fig. S38**. The plots of optical constants.
Page 44, **References**.

Table S1. Optimized equilibrium lattice constant (a (Å)), bulk modulus (B_0 (GPa)), and its pressure derivative (B_0') for novel materials $(X_4Y)(O_2B-C_{12}H_6-BO_2)_3$ ($X=C/Si$; $Y=C, Si, Ge, Sn, \text{ and } Pb$) as well as prototypical MOF-5.

(X, Y)	a (Å)	B_0 (GPa) ^a	B_0' ^a
(C, C)	24.4264	22.62(22.64)[22.64]	3.64(3.66)[3.67]
(C, Si)	24.6751	21.75(21.77)[21.77]	3.73(3.74)[3.74]
(C, Ge)	24.7173	21.68(21.70)[21.69]	2.99(3.01)[2.99]
(C, Sn)	24.8698	21.16(21.18)[21.18]	3.60(3.62)[3.62]
(C, Pb)	24.9207	21.14(21.15)[21.15]	3.08(3.10)[3.11]
(Si, C)	25.8190	19.44(19.45)[19.44]	2.33(2.35)[2.35]
(Si, Si)	26.1963	18.63(18.64)[18.64]	3.32(3.34)[3.33]
(Si, Ge)	26.2123	18.55(18.56)[18.57]	3.63(3.65)[3.66]
(Si, Sn)	26.3780	18.00(18.01)[18.02]	3.49(3.51)[3.50]
(Si, Pb)	26.4125	17.96(17.97)[17.97]	3.54(3.55)[3.55]
MOF-5	$\langle 25.6690 \rangle^b \langle 25.8849 \rangle^c 26.0443^d$	15.37(15.37)[15.37] ^d	5.06(5.13)[5.17] ^d

^aData without brackets from Murnaghan EOS; data (in parentheses) from Birch-Murnaghan 3rd-order EOS; data [in brackets] from Universal EOS. ^b and ^c The lattice parameters of single crystals of as-synthesized and fully desolvated MOF-5 from ref¹, respectively. ^dThe calculated lattice parameter and bulk modulus of MOF-5 from PAW-PBE VASP calculations in ref².

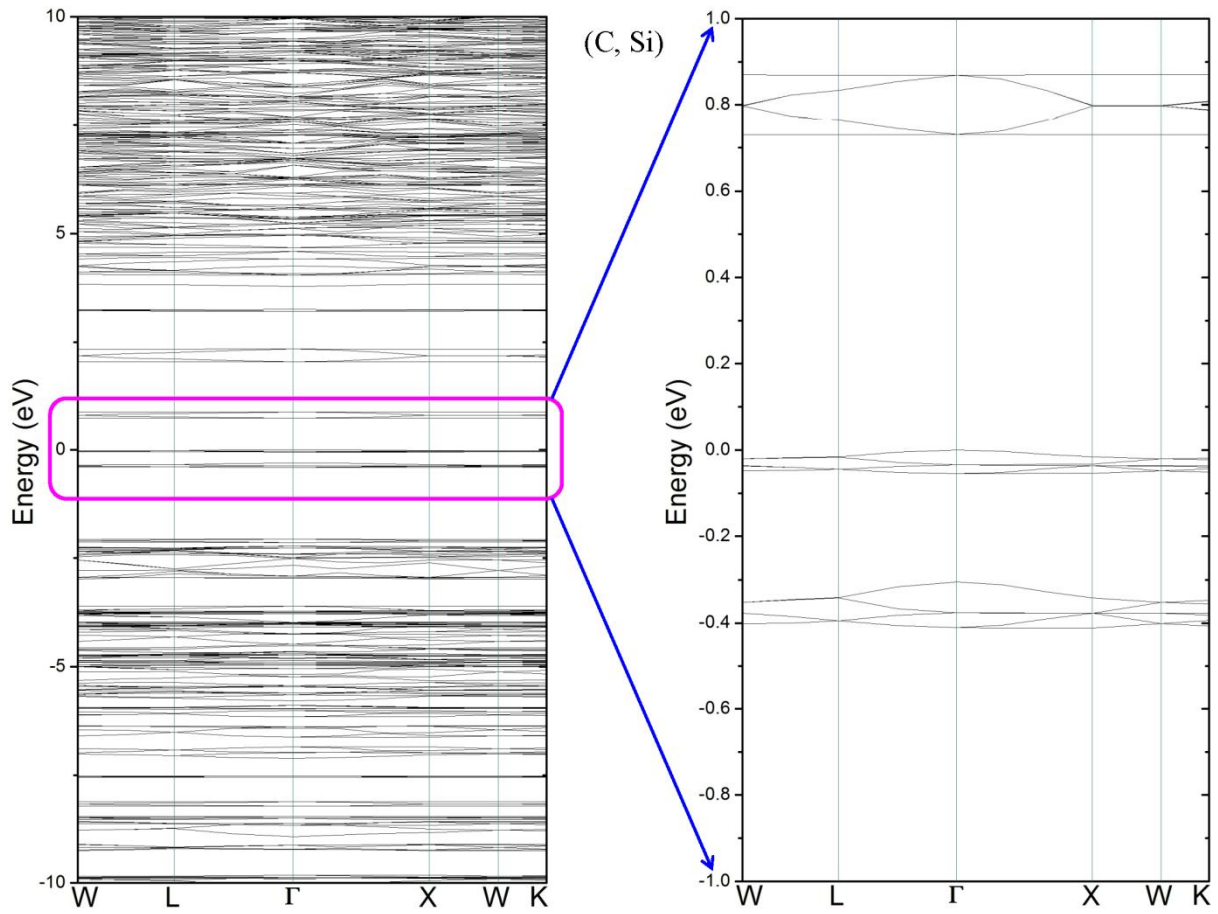


Figure S1. The electronic band structure of (C, Si). The Fermi level is set to zero and placed in the valence band maximum.

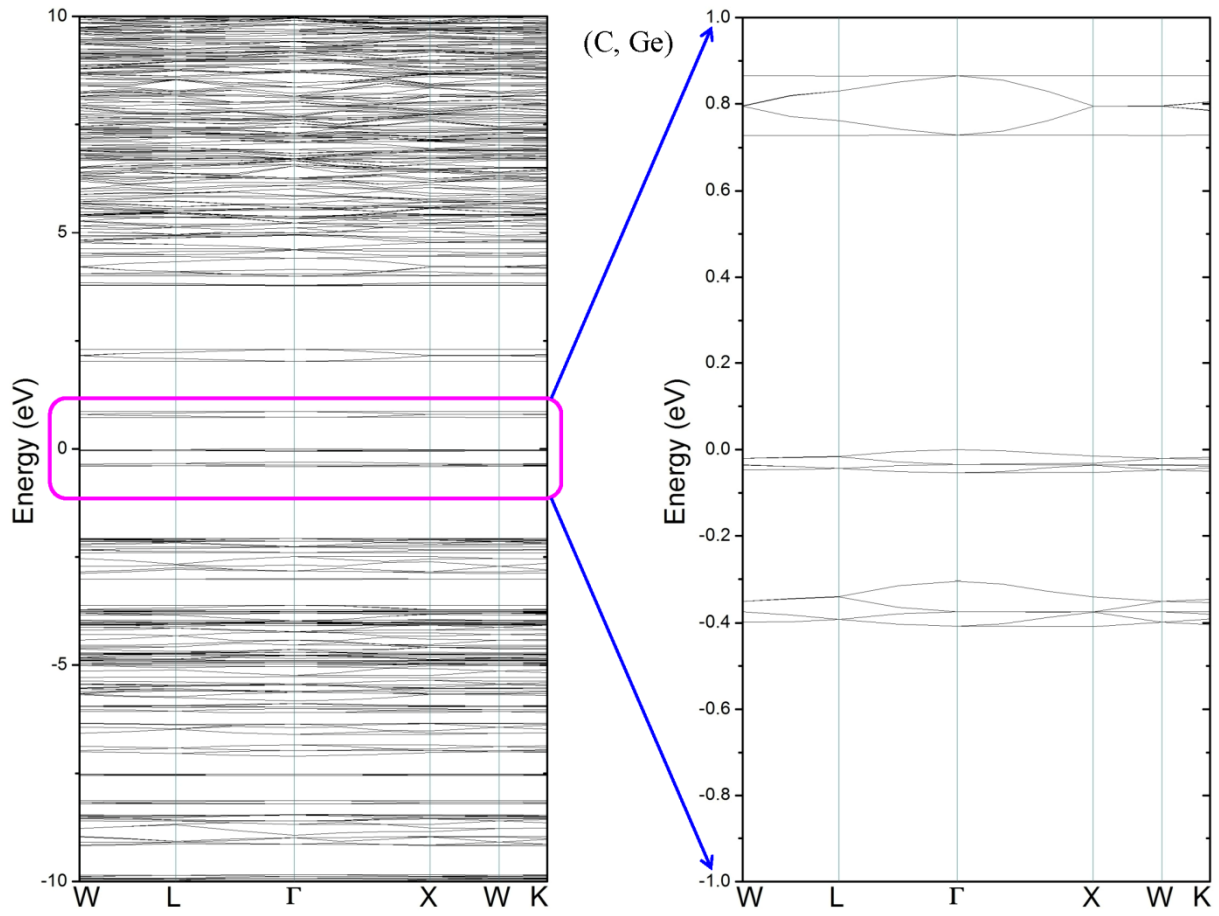


Figure S2. The electronic band structure of (C, Ge). The Fermi level is set to zero and placed in the valence band maximum.

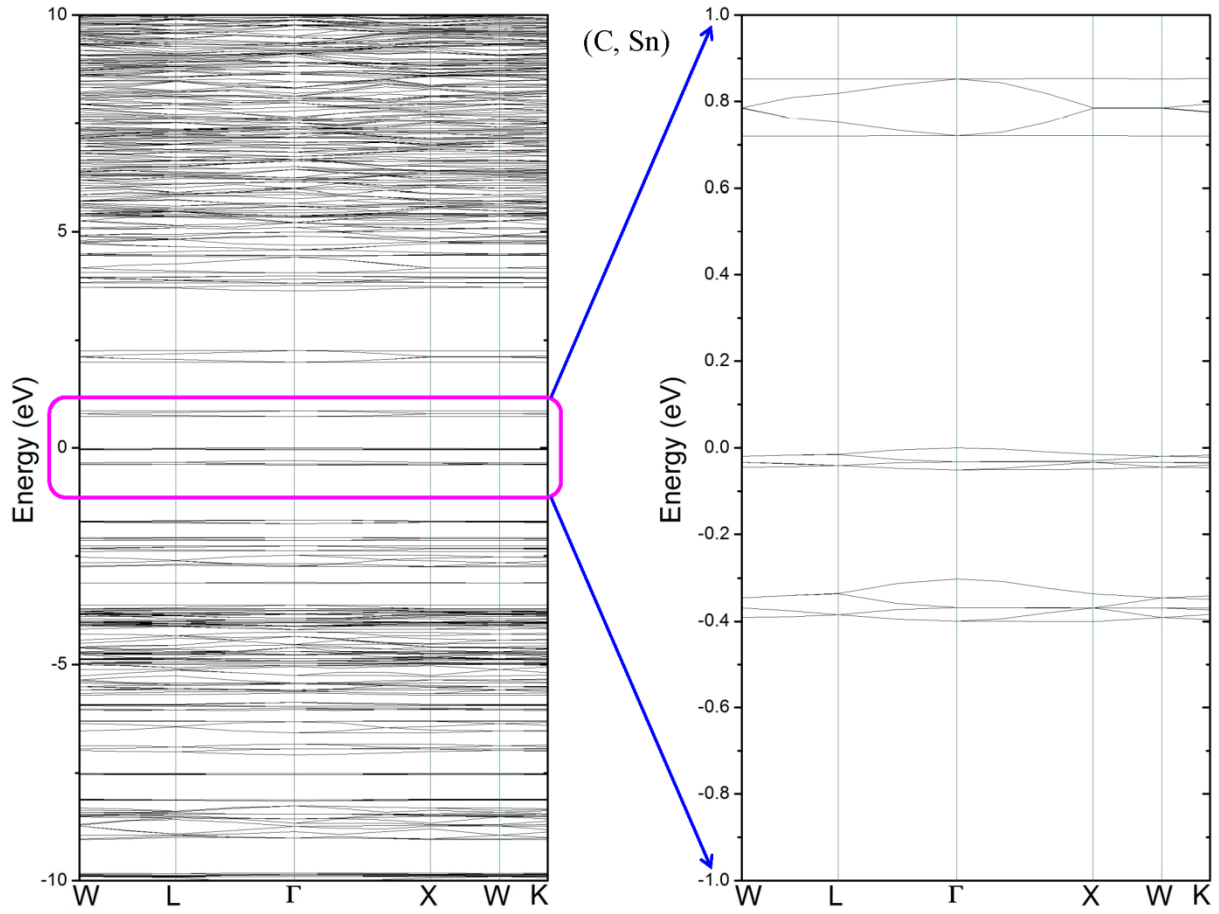


Figure S3. The electronic band structure of (C, Sn). The Fermi level is set to zero and placed in the valence band maximum.

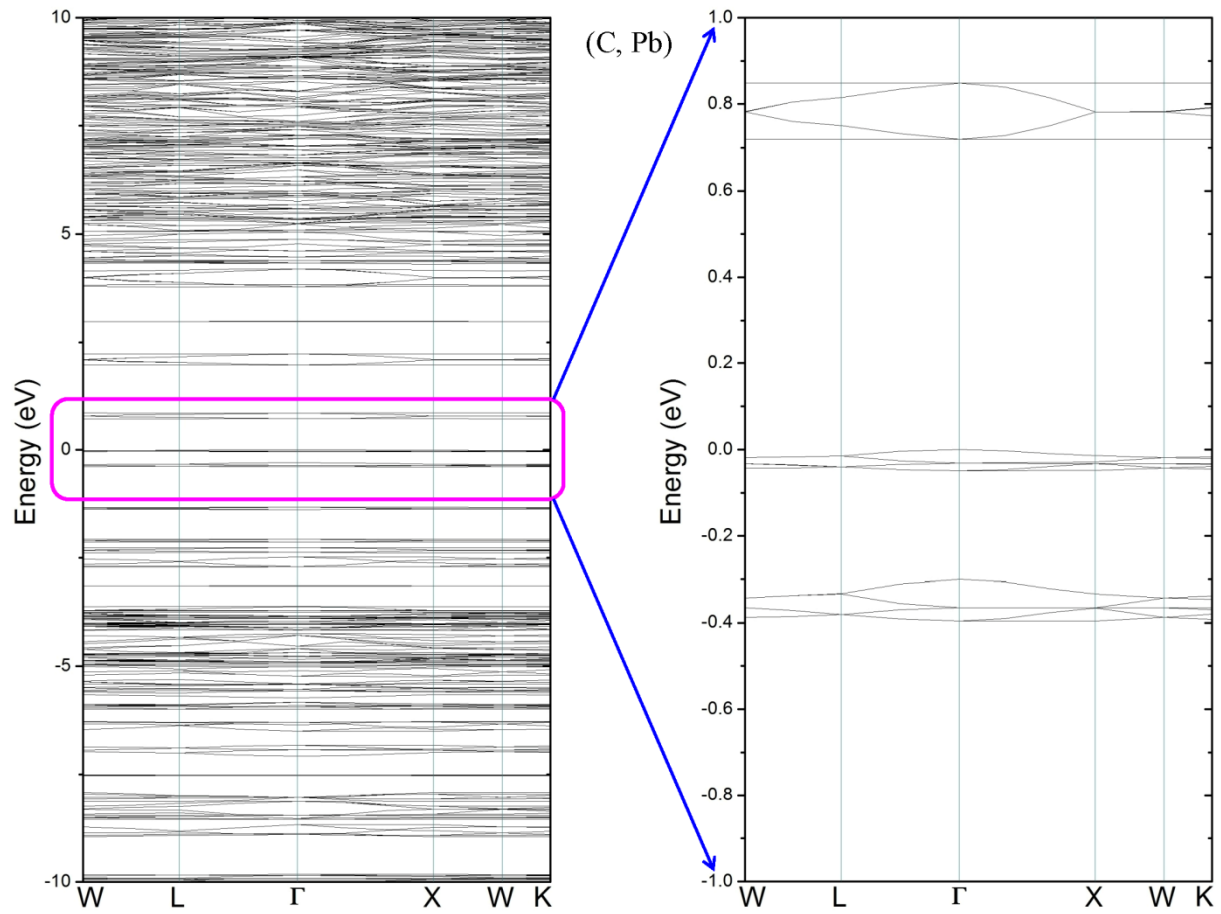


Figure S4. The electronic band structure of (C, Pb). The Fermi level is set to zero and placed in the valence band maximum.

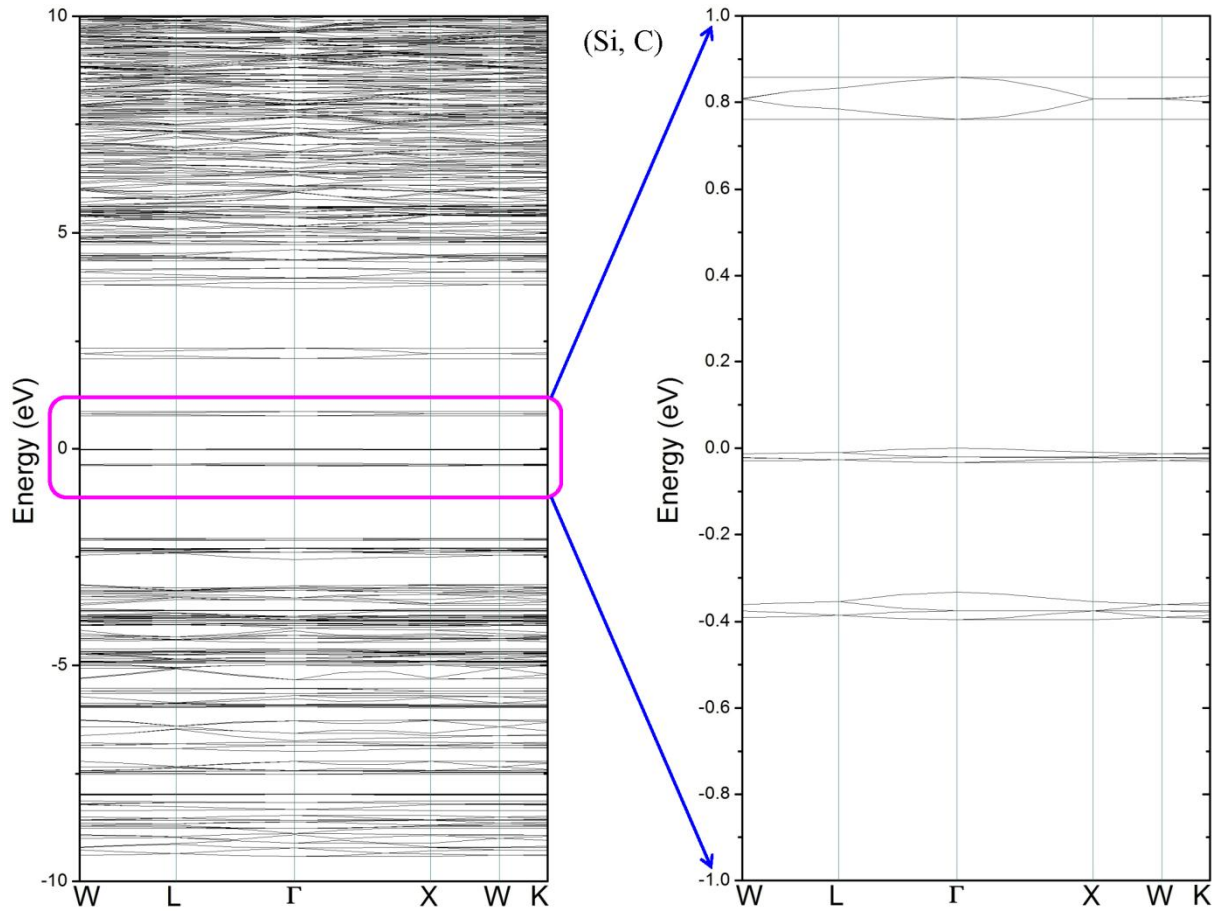


Figure S5. The electronic band structure of (Si, C). The Fermi level is set to zero and placed in the valence band maximum.

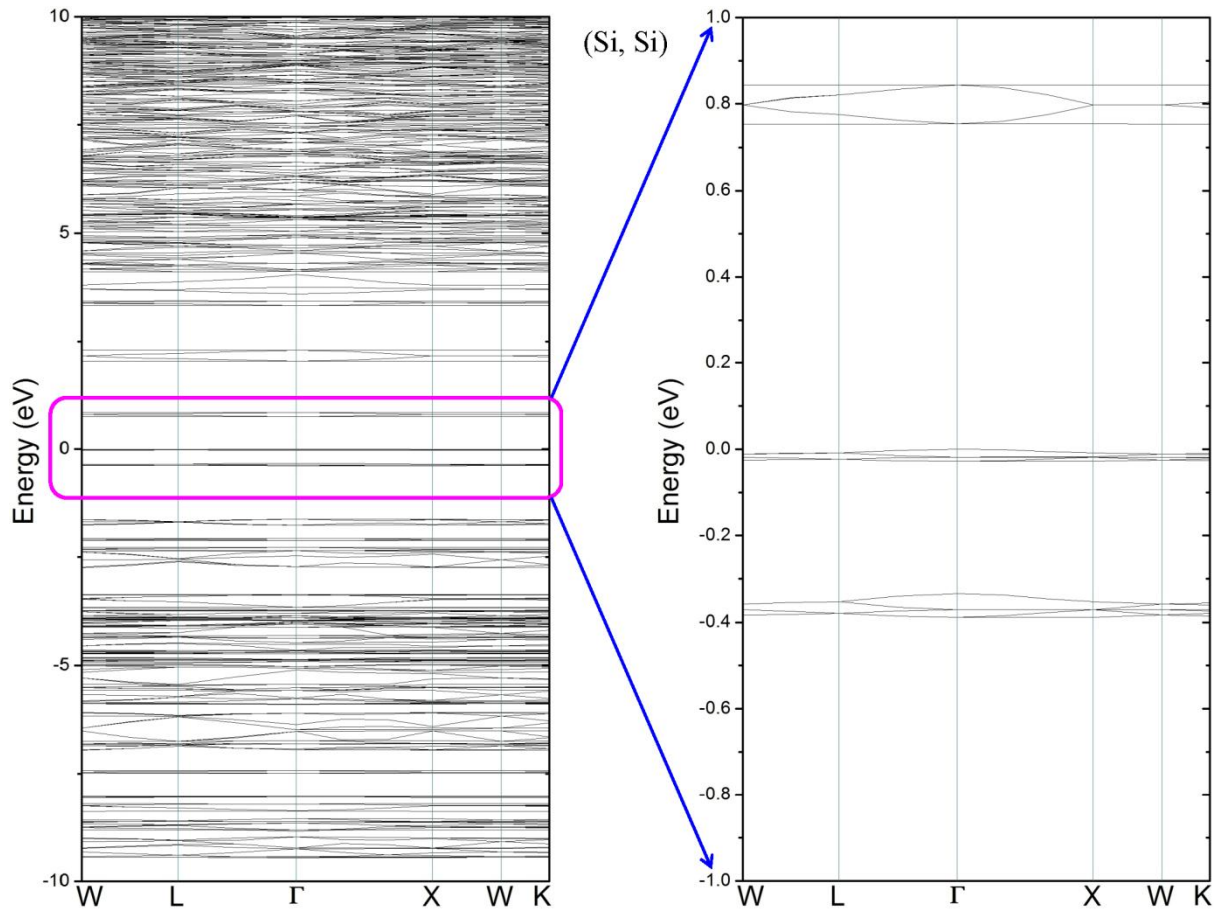


Figure S6. The electronic band structure of (Si, Si). The Fermi level is set to zero and placed in the valence band maximum.

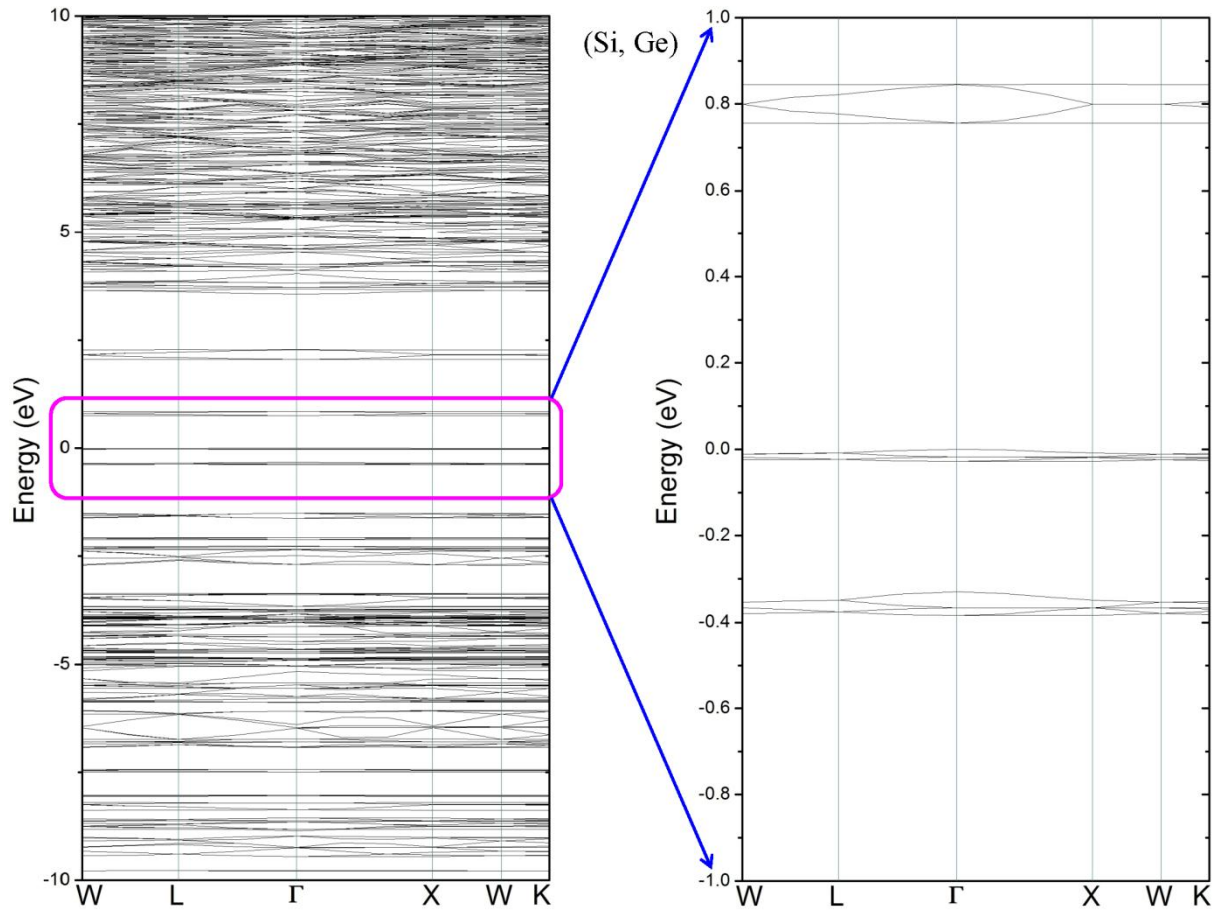


Figure S7. The electronic band structure of (Si, Ge). The Fermi level is set to zero and placed in the valence band maximum.

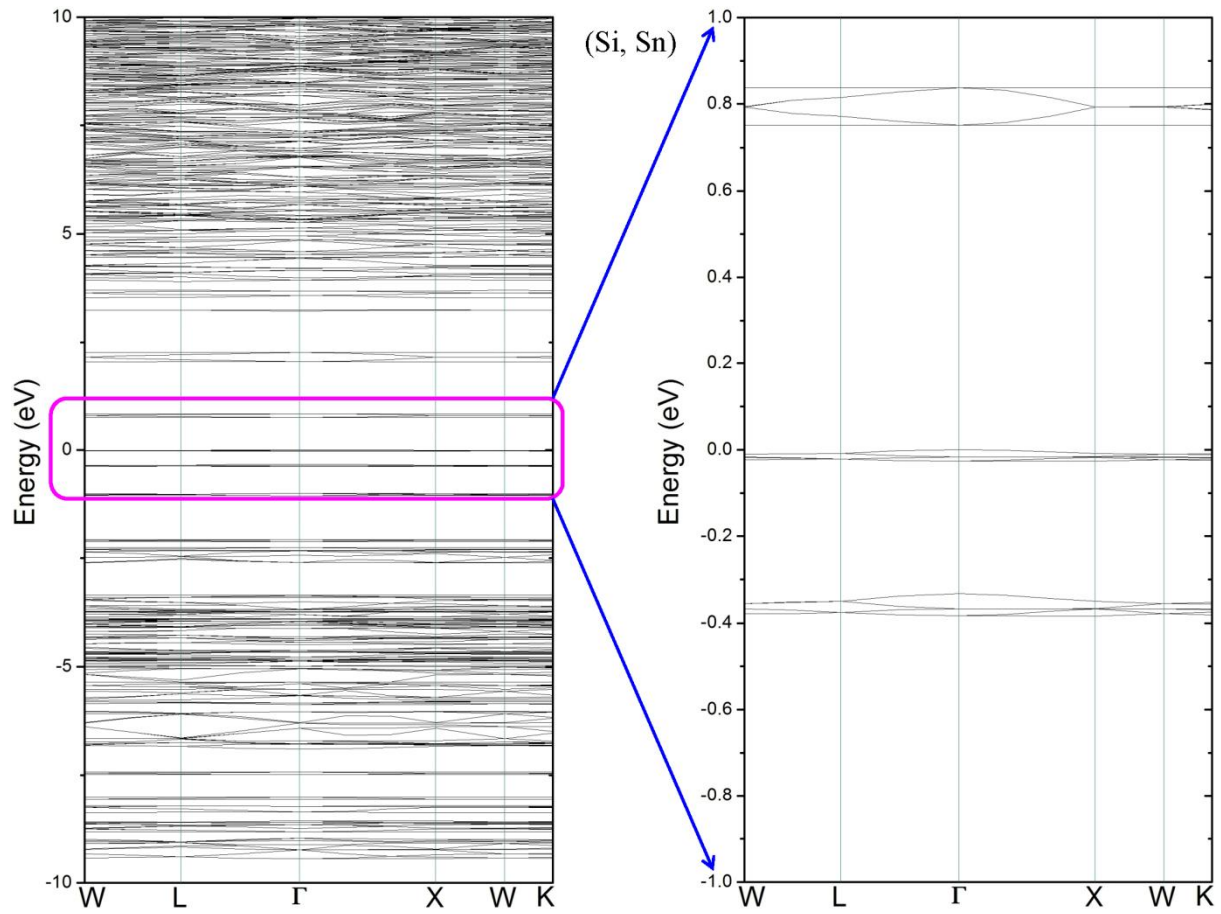


Figure S8. The electronic band structure of (Si, Sn). The Fermi level is set to zero and placed in the valence band maximum.

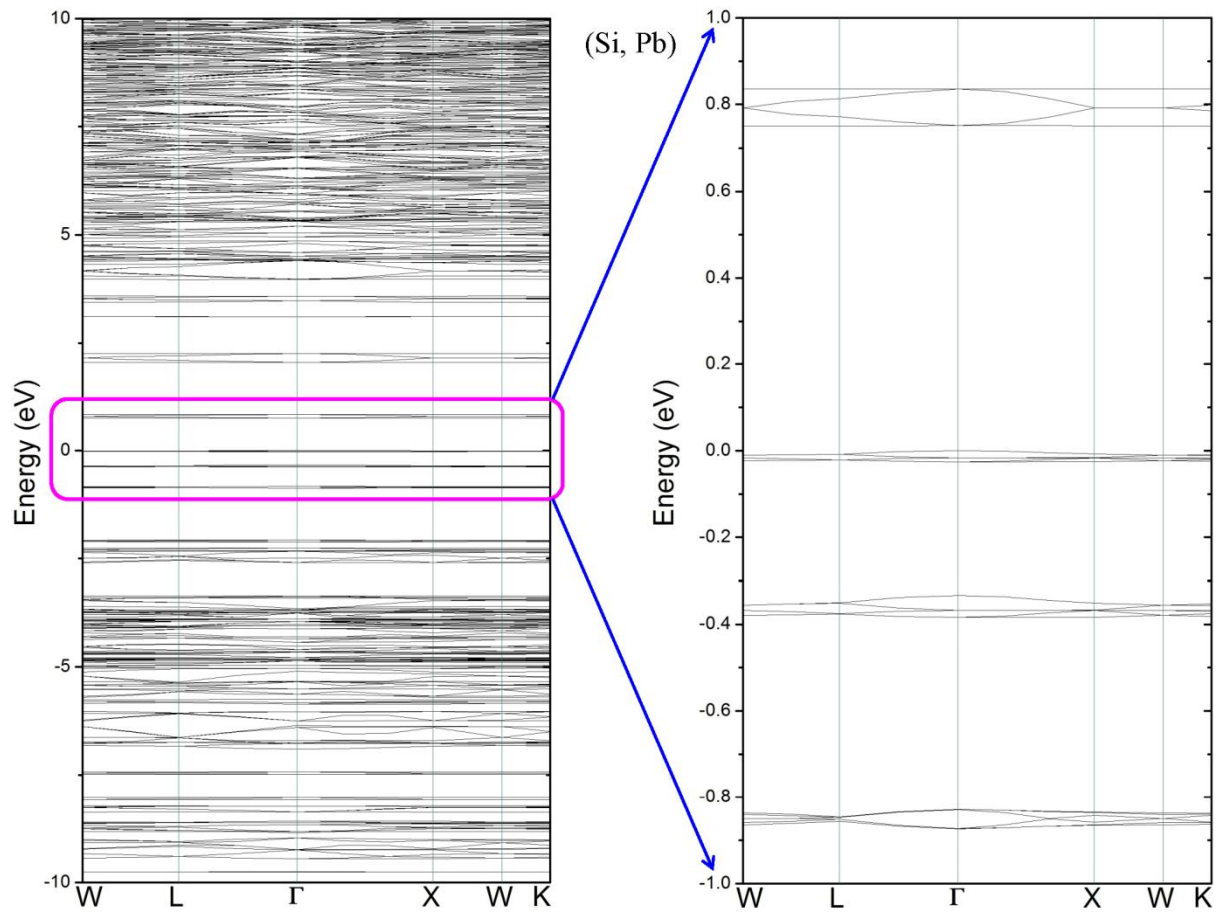


Figure S9. The electronic band structure of (Si, Pb). The Fermi level is set to zero and placed in the valence band maximum.

Table S2. Estimated band gap values (Theo. E_g (in eV)) for the novel materials $(X_4Y)(O_2B-C_{12}H_6-BO_2)_3$ ($X = C/Si$; $Y = C, Si, Ge, Sn,$ and Pb), experimental and theoretical band gap values (Exp. E_g) for prototypical MOF-5, as well as the corresponding wavelength (λ in nm) of absorption lights. Note that $\lambda = hc/E$ in nm; h is Planck constant (in eV·s), c is the speed of light (i.e., 3×10^8 m/s or 3×10^{17} nm/s), E is the energy (in eV), here corresponding to a certain band gap of a specific material.

(X, Y)	E_g^1	λ^1	E_g^2	λ^2	E_g^3	λ^3
(C, C)	0.736	1685.7	1.235	1005.0	1.375	902.5
(C, Si)	0.729	1701.9	1.162	1068.1	0.886	1399.7
(C, Ge)	0.727	1706.6	1.158	1071.1	1.469	844.6
(C, Sn)	0.721	1720.8	1.122	1105.8	1.391	892.2
(C, Pb)	0.718	1728.0	1.107	1120.7	0.754	1644.7
(Si, C)	0.760	1632.5	1.224	1013.4	1.386	895.1
(Si, Si)	0.753	1647.7	1.189	1043.2	1.049	1182.6
(Si, Ge)	0.755	1643.3	1.201	1032.7	1.284	966.6
(Si, Sn)	0.751	1652.1	1.199	1034.9	0.967	1283.4
(Si, Pb)	0.750	1654.3	1.202	1031.9	0.857	1447.3
MOF-5	3.558 ^a	348.7				
MOF-5	3.4-4.0 ^b	364.9-310.2				

^aThe theoretical band gap of MOF-5 and threshold absorption wavelength, from ref.^{2,3}

^bThe experimental band gaps of MOF-5 and threshold absorption wavelength, from ref.⁴⁻⁶

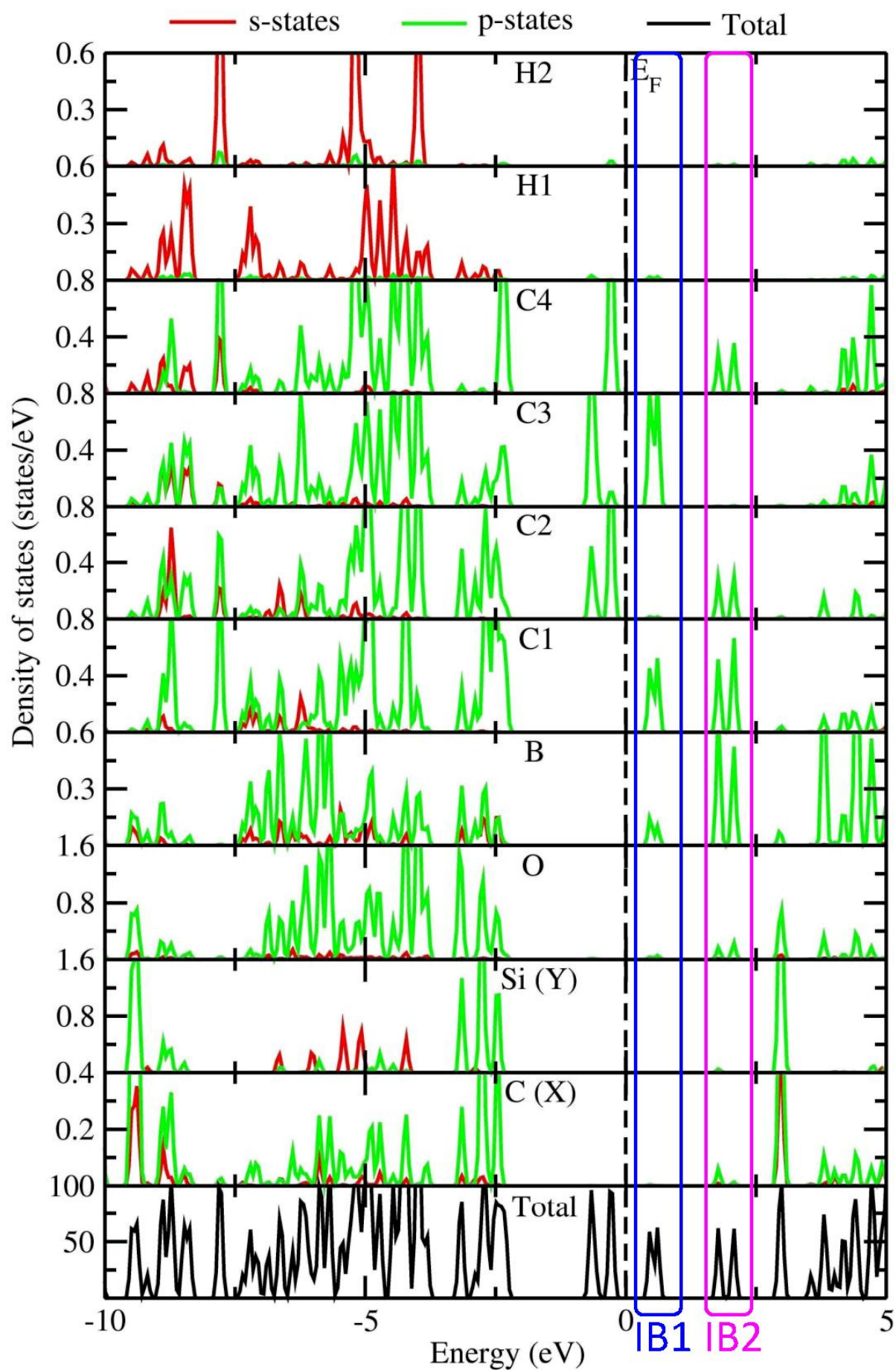


Figure S10. The calculated total density of states (TDOS) and partial density of states (PDOS) for (C, Si) in the cubic $Fm-3m$ symmetry (no. 225)

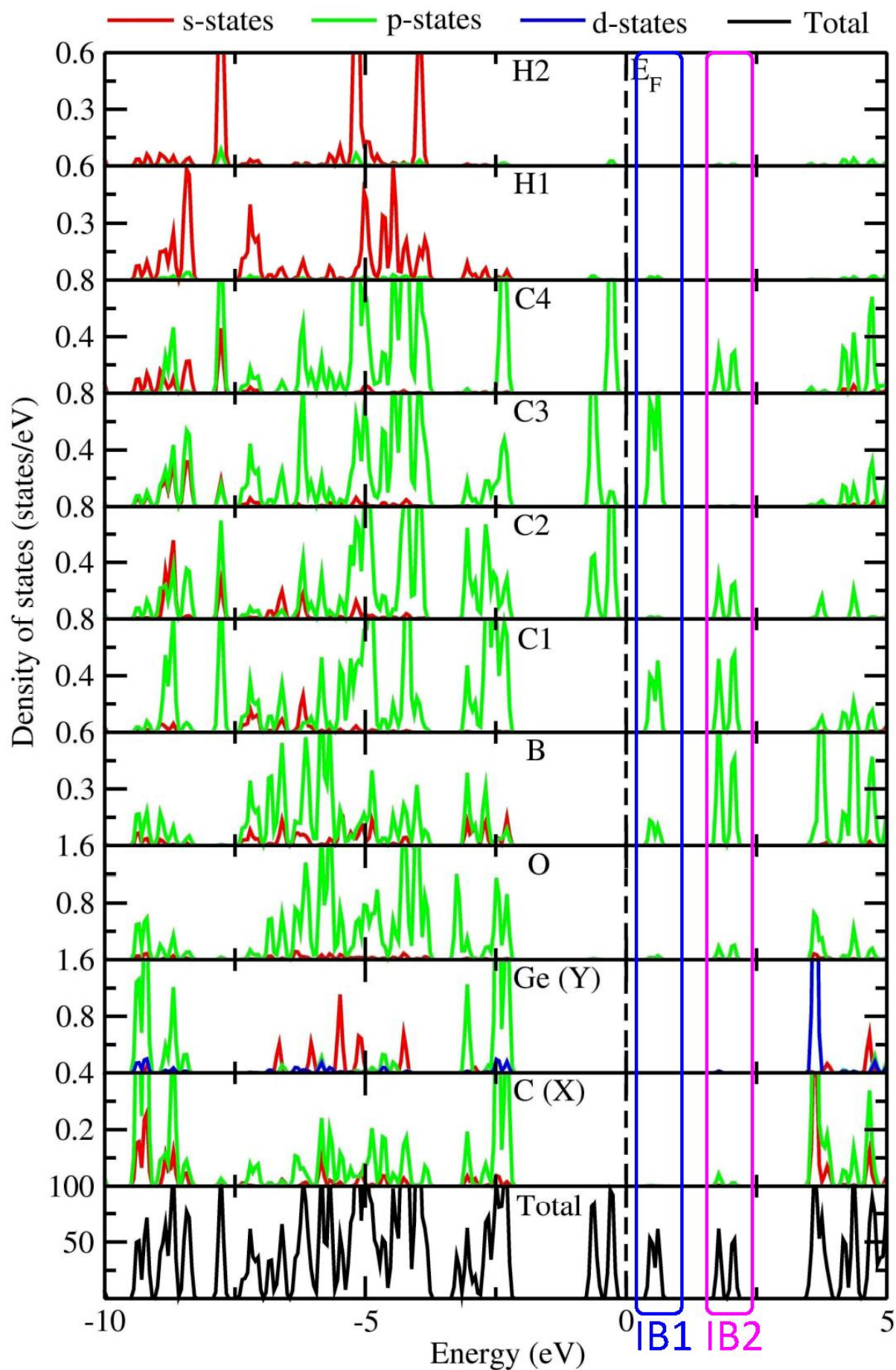


Figure S11. The calculated total density of states (TDOS) and partial density of states (PDOS) for (C, Ge) in the cubic $Fm-3m$ symmetry (no. 225)

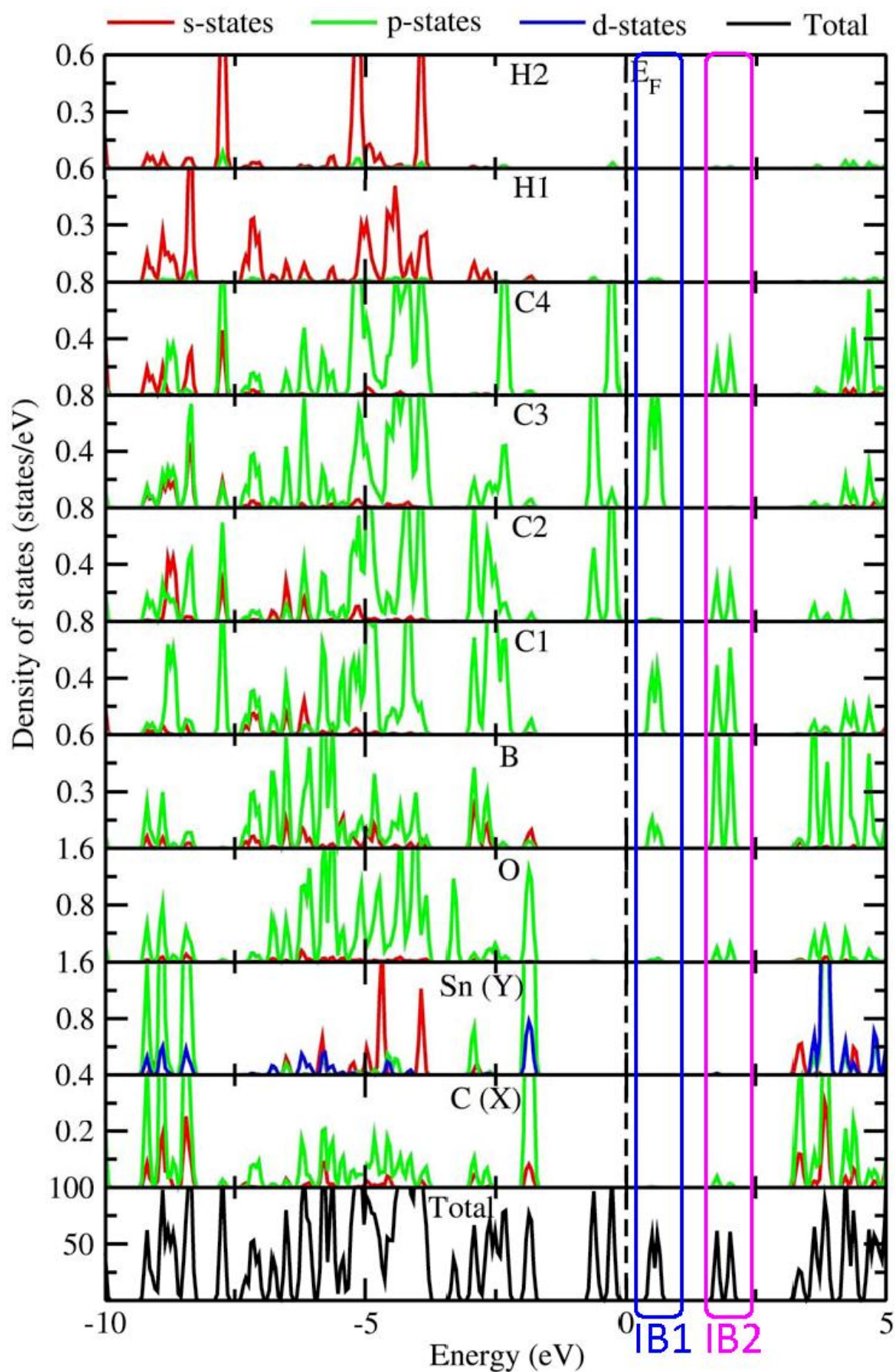


Figure S12. The calculated total density of states (TDOS) and partial density of states (PDOS) for (C, Sn) in the cubic $Fm\bar{3}m$ symmetry (no. 225)

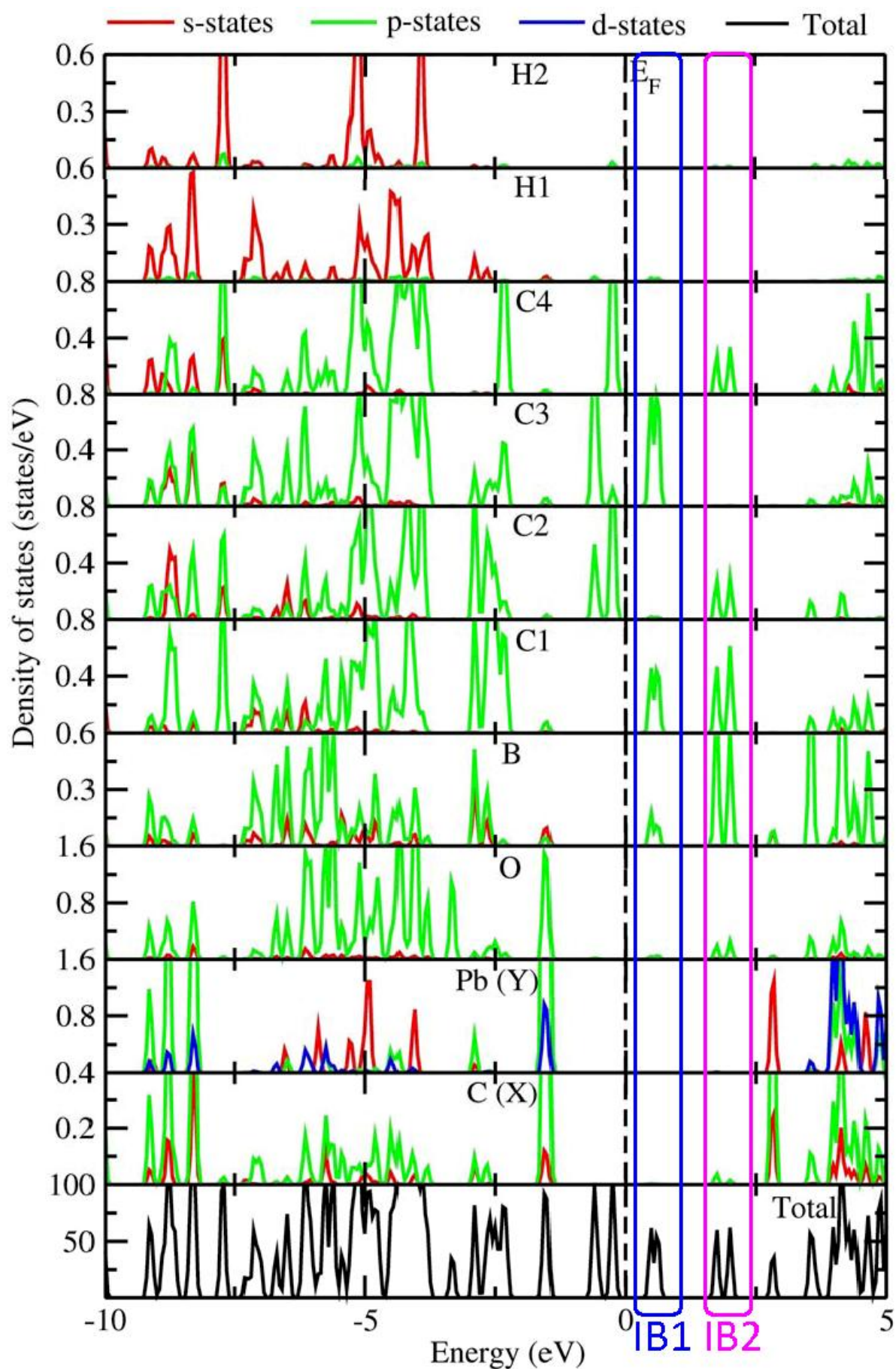


Figure S13. The calculated total density of states (TDOS) and partial density of states (PDOS) for (C, Pb) in the cubic $Fm-3m$ symmetry (no. 225)

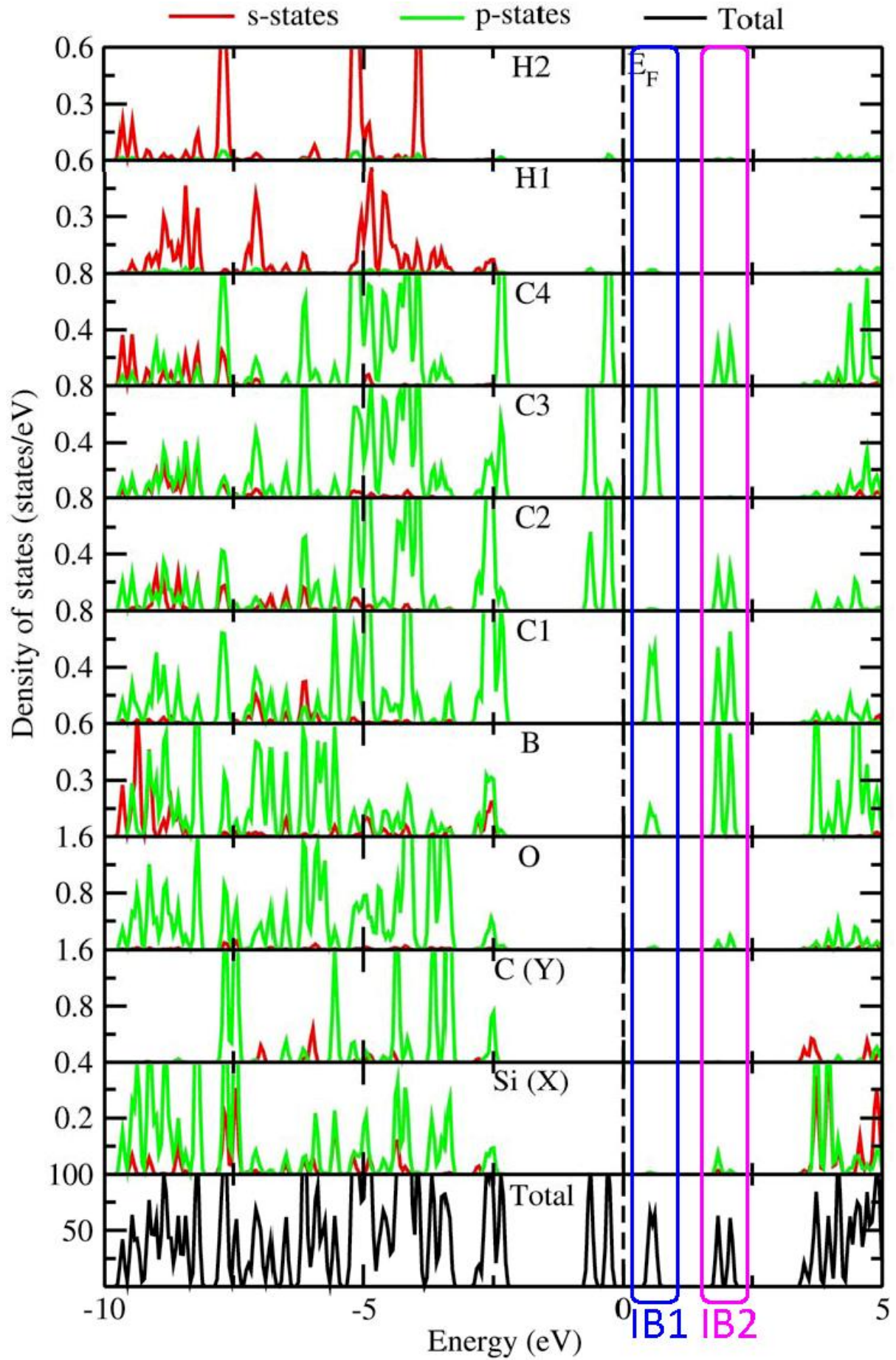


Figure S14. The calculated total density of states (TDOS) and partial density of states (PDOS) for (Si, C) in the cubic $Fm-3m$ symmetry (no. 225)

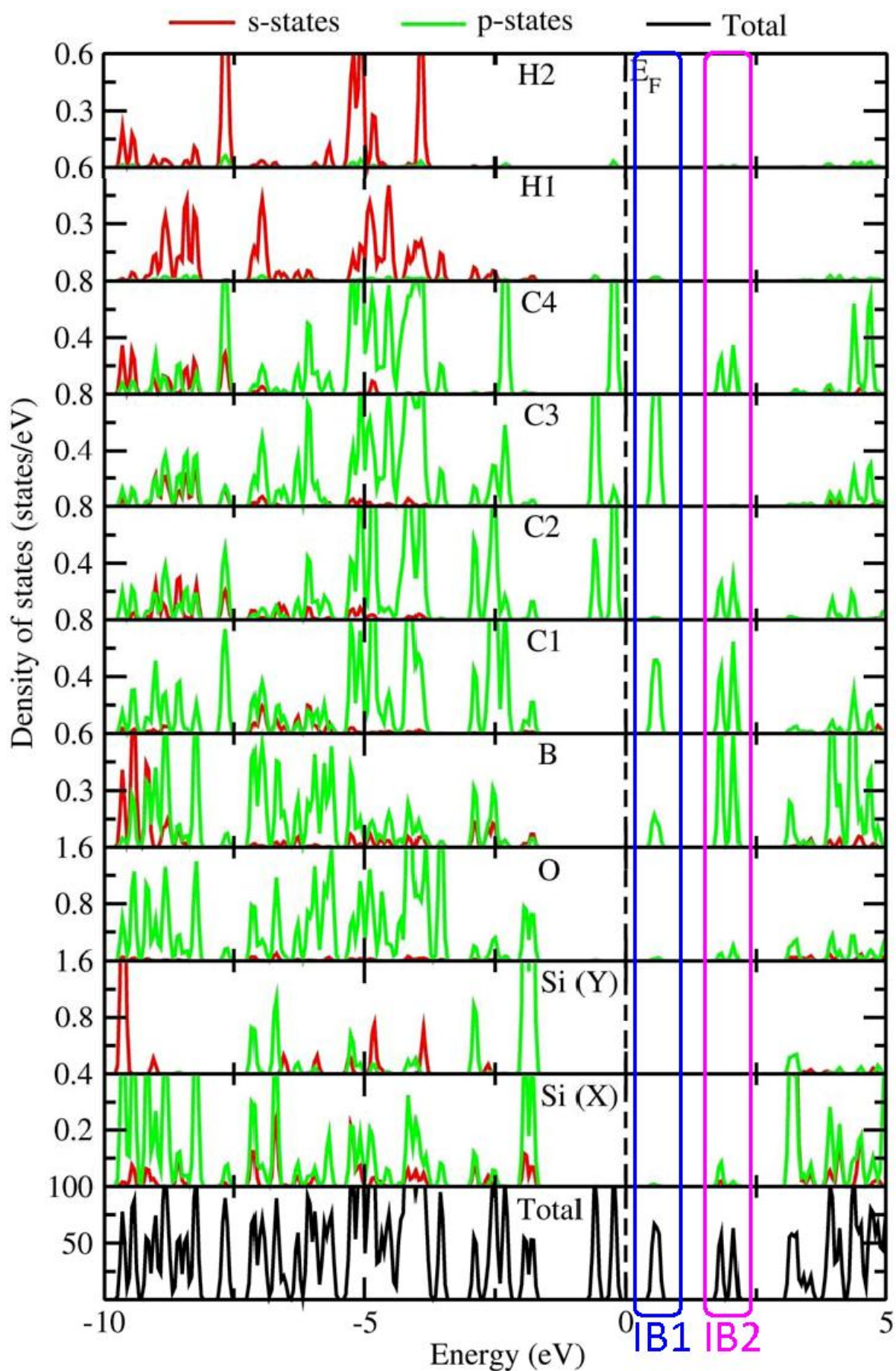


Figure S15. The calculated total density of states (TDOS) and partial density of states (PDOS) for (Si, Si) in the cubic $Fm-3m$ symmetry (no. 225)

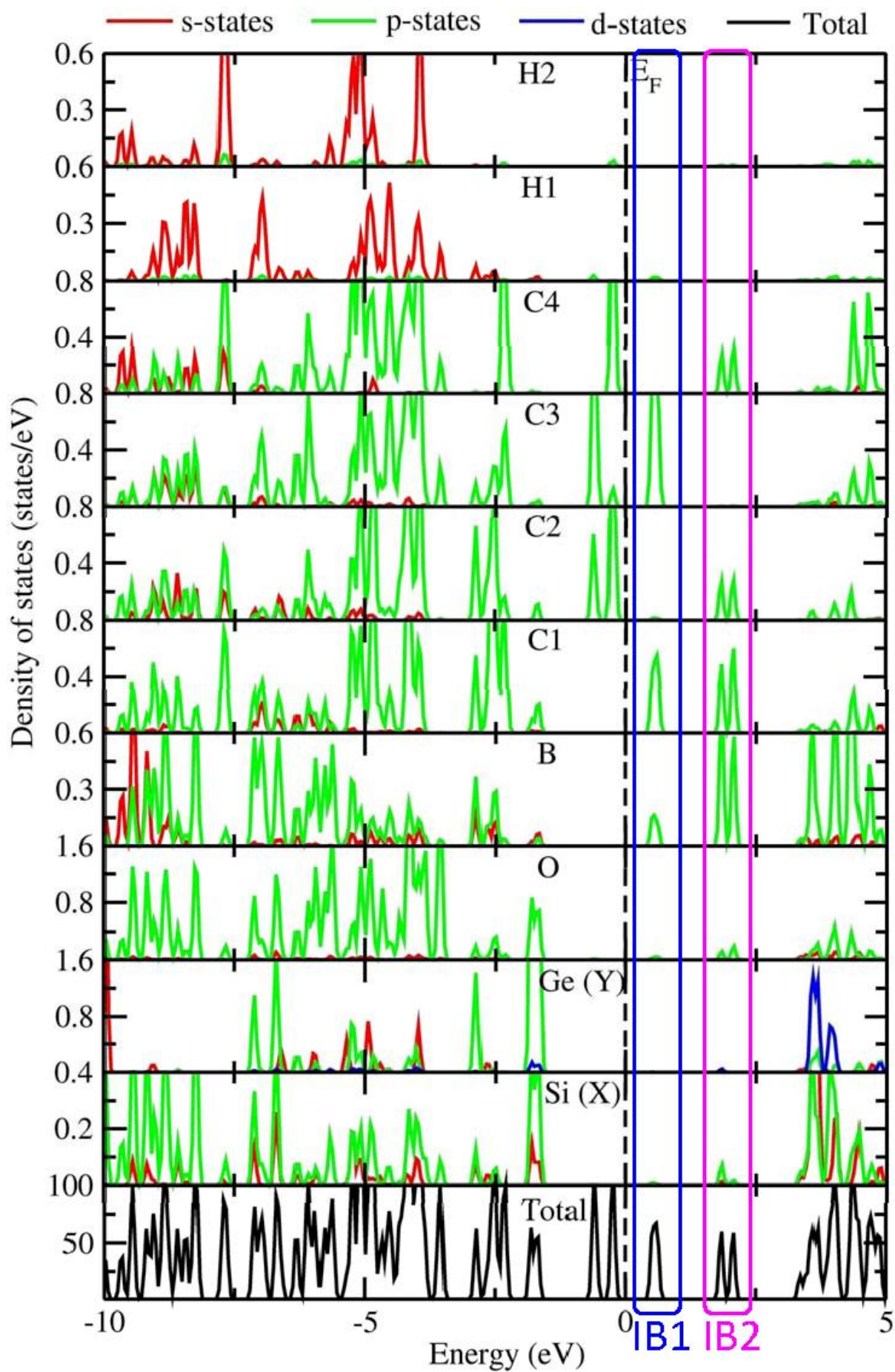


Figure S16. The calculated total density of states (TDOS) and partial density of states (PDOS) for (Si, Ge) in the cubic $Fm-3m$ symmetry (no. 225)

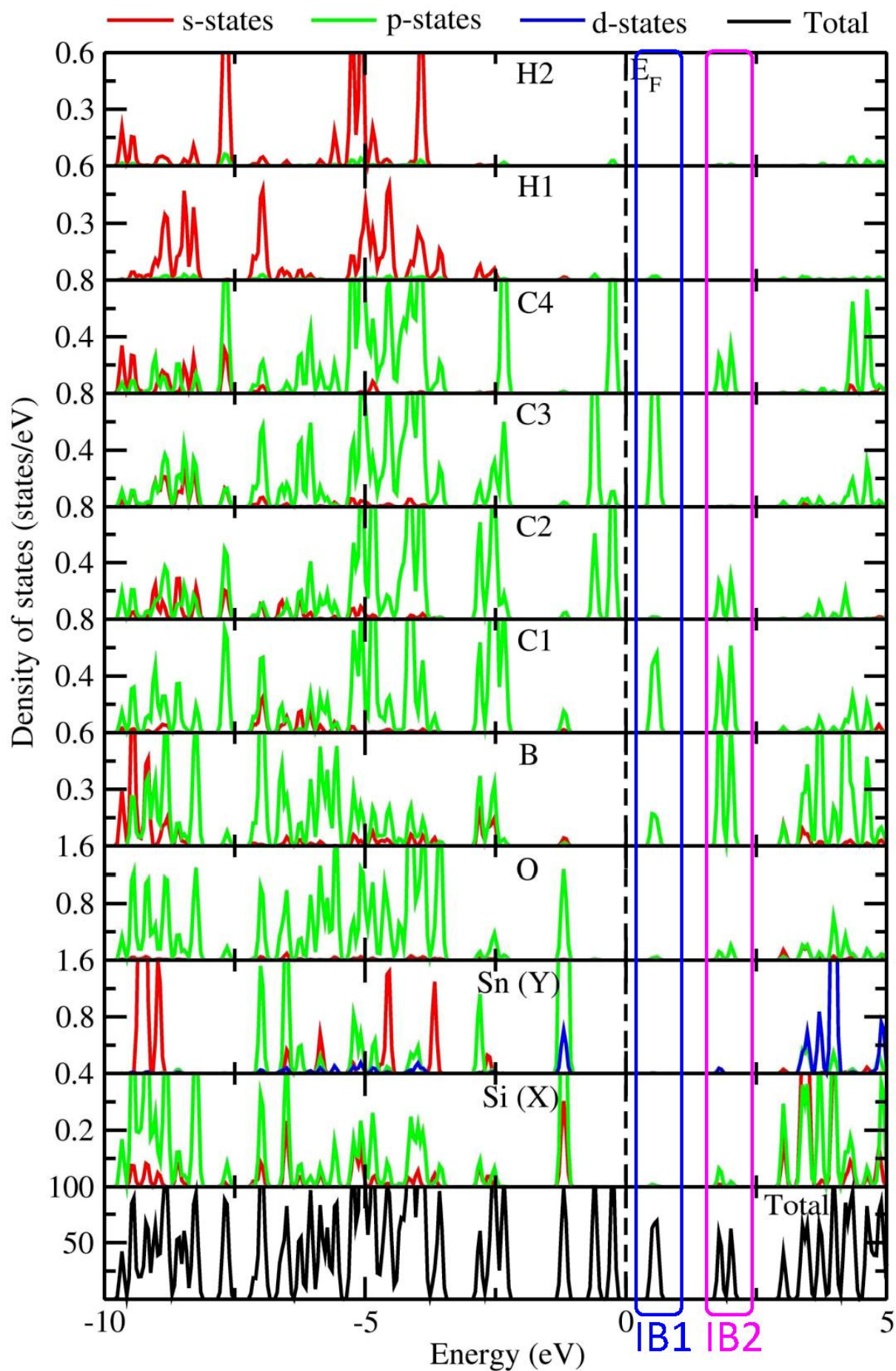


Figure S17. The calculated total density of states (TDOS) and partial density of states (PDOS) for (Si, Sn) in the cubic $Fm-3m$ symmetry (no. 225)

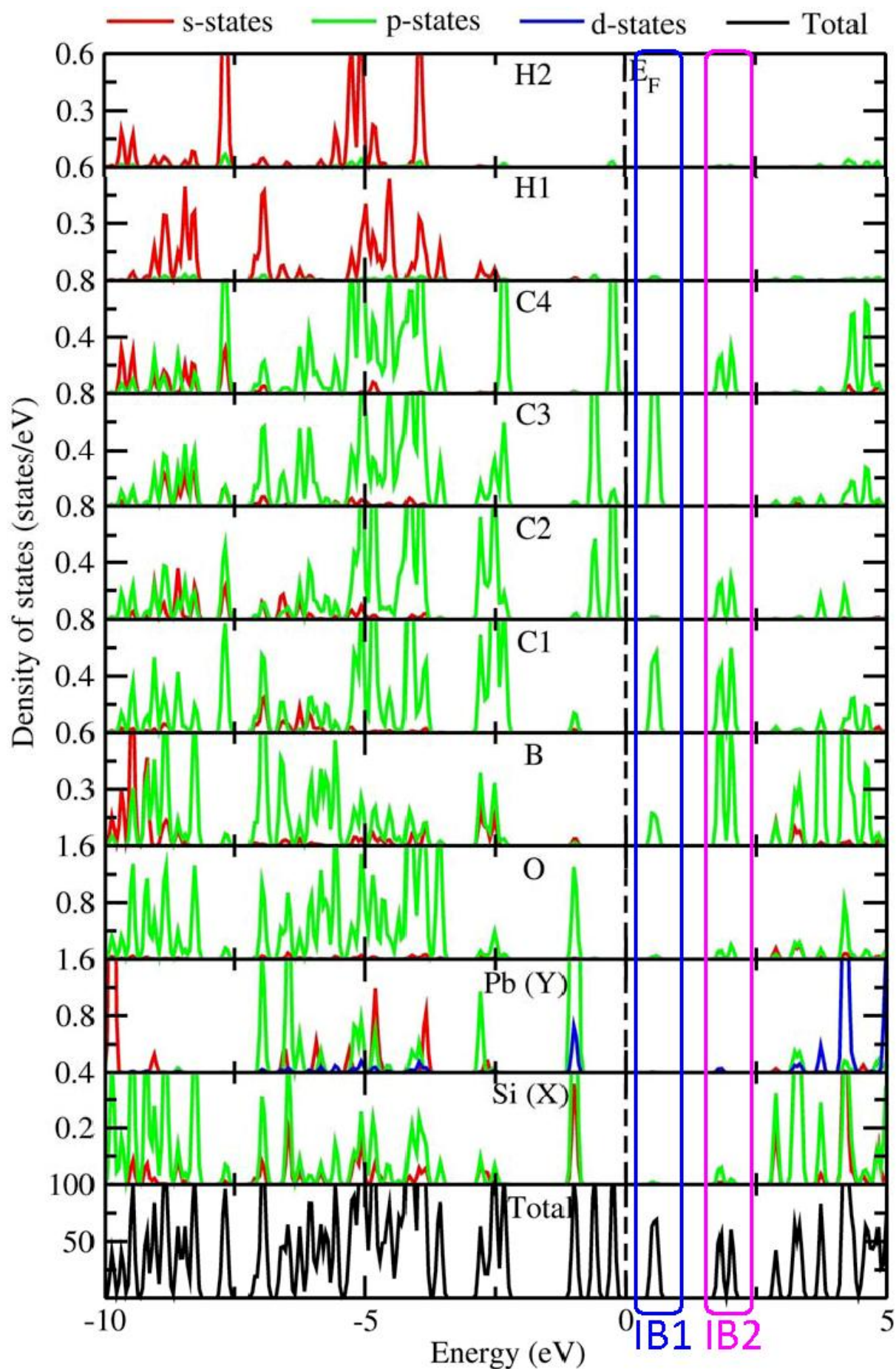
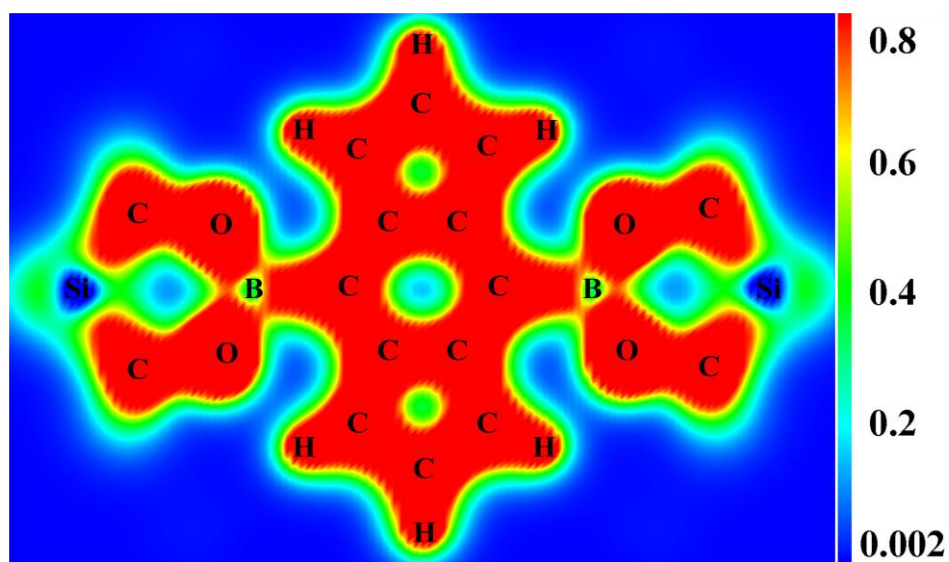
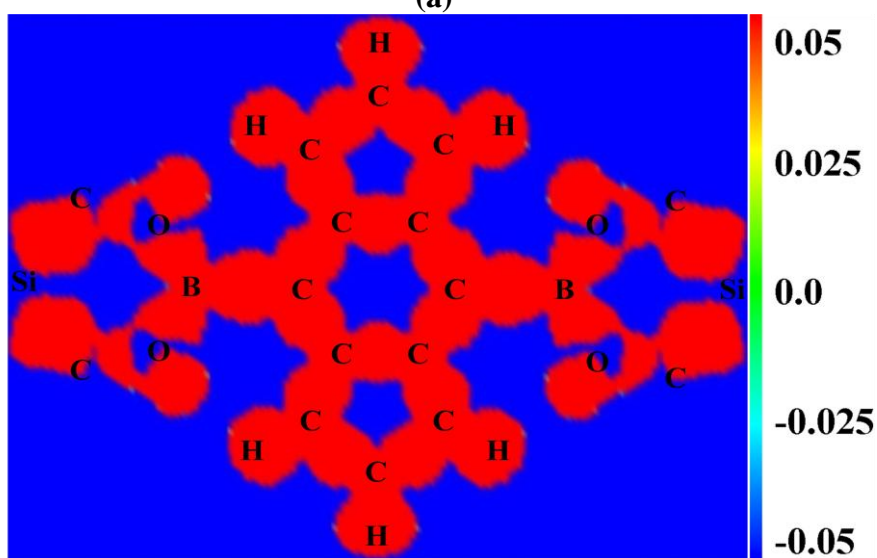


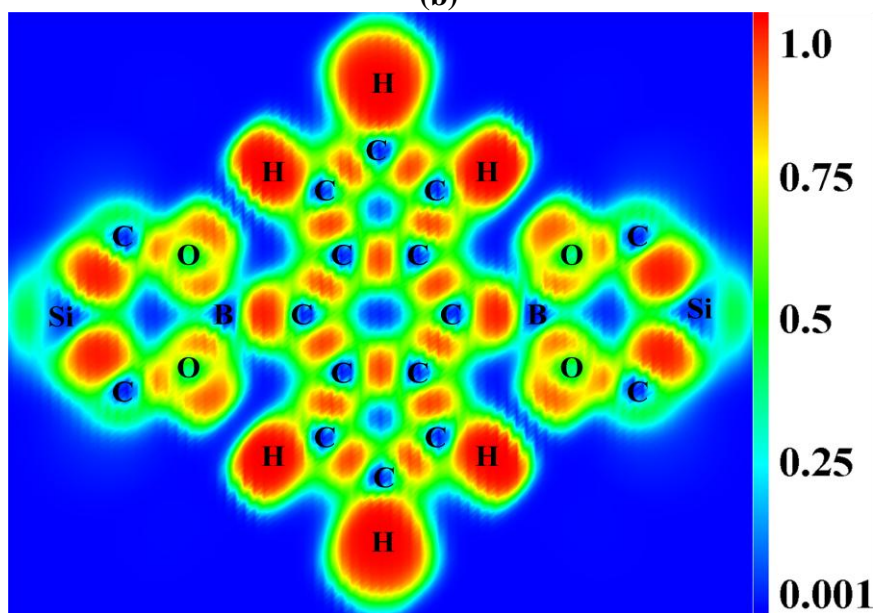
Figure S18. The calculated total density of states (TDOS) and partial density of states (PDOS) for (Si, Pb) in the cubic $Fm-3m$ symmetry (no. 225)



(a)

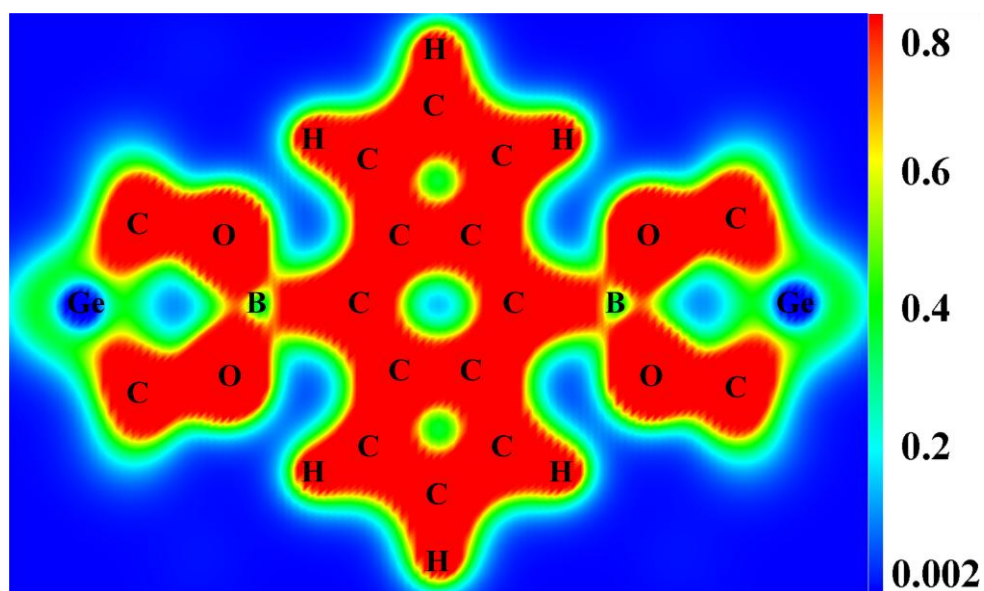


(b)

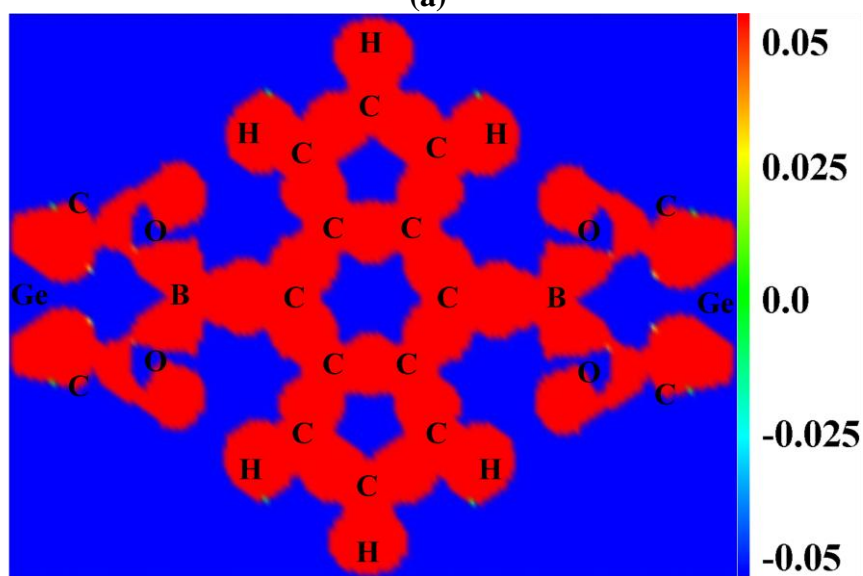


(c)

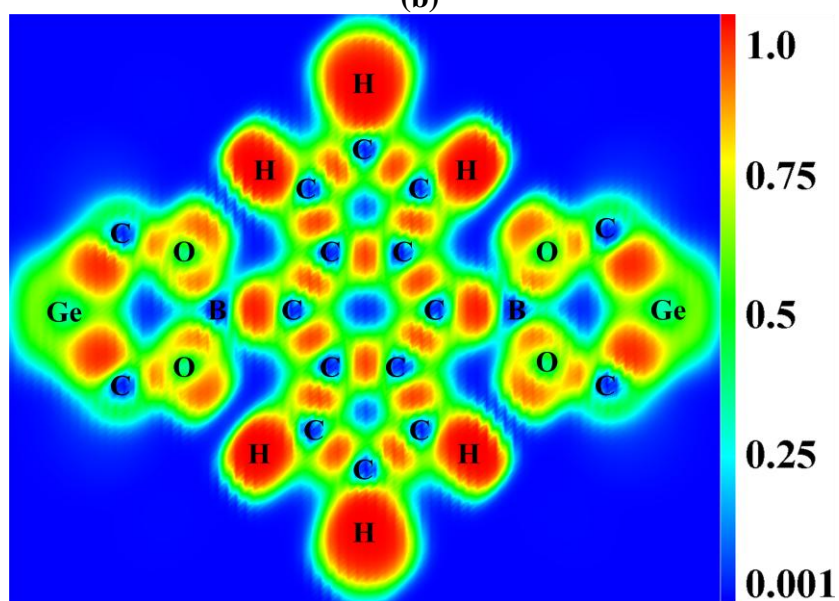
Figure S19. Calculated charge density (a) in $e/\text{\AA}^3$, charge transfer (b) in $e/\text{\AA}^3$, and electron localization function (c) plots for (C, Si) in the (110) plane.



(a)

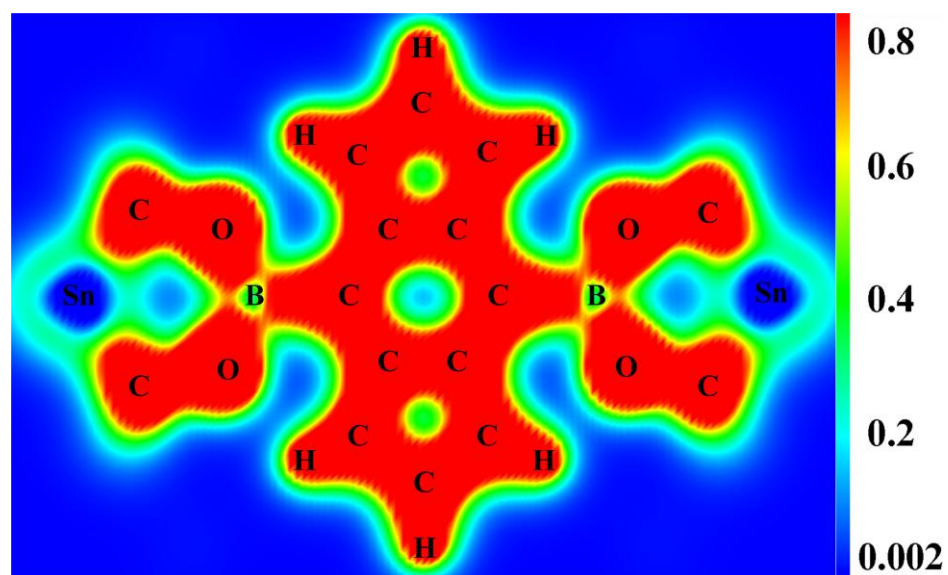


(b)

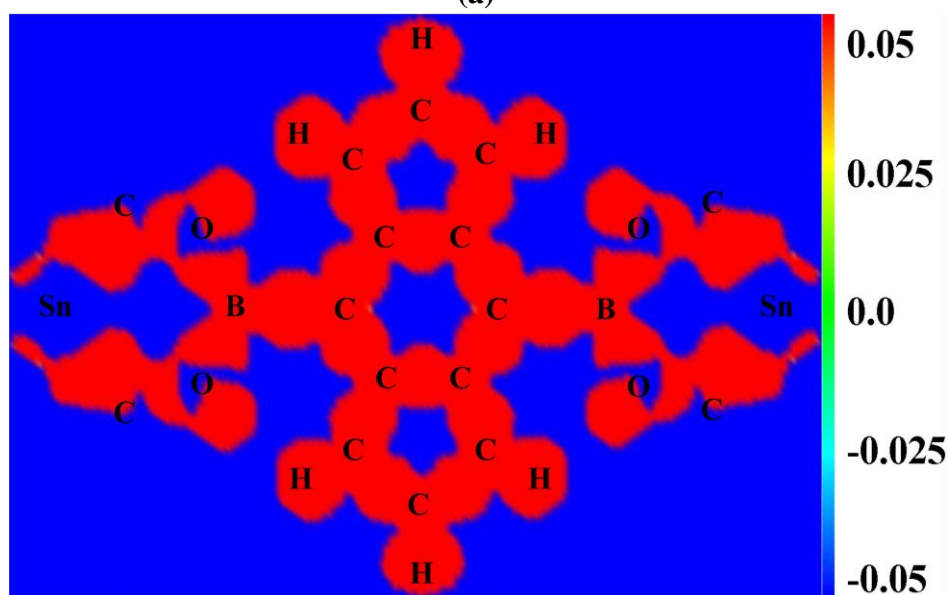


(c)

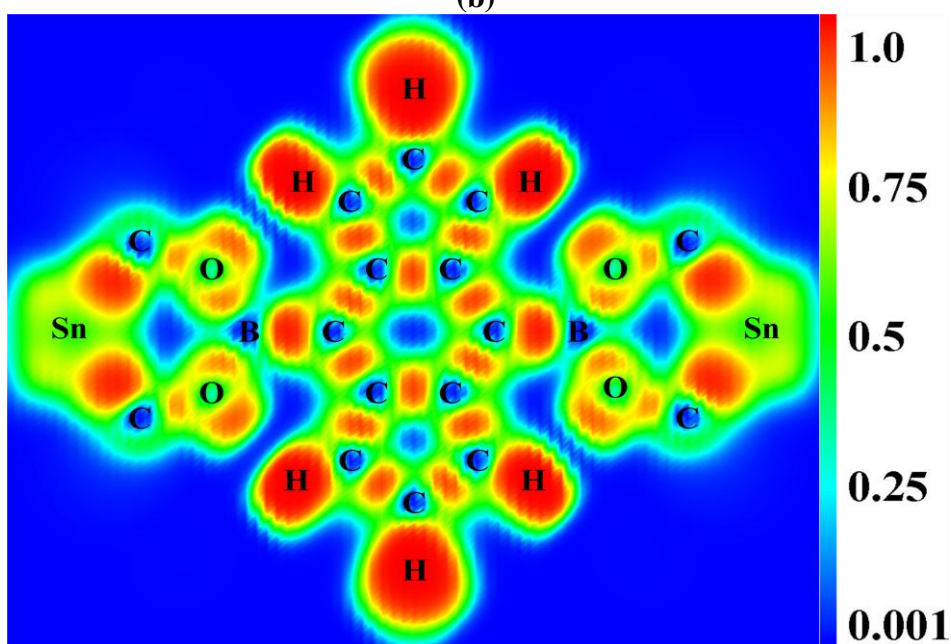
Figure S20. Calculated charge density (a) in $e/\text{\AA}^3$, charge transfer (b) in $e/\text{\AA}^3$, and electron localization function (c) plots for (C, Ge) in the (110) plane.



(a)



(b)



(c)

Figure S21. Calculated charge density (a) in $e/\text{\AA}^3$, charge transfer (b) in $e/\text{\AA}^3$, and electron localization function (c) plots for (C, Sn) in the (110) plane.

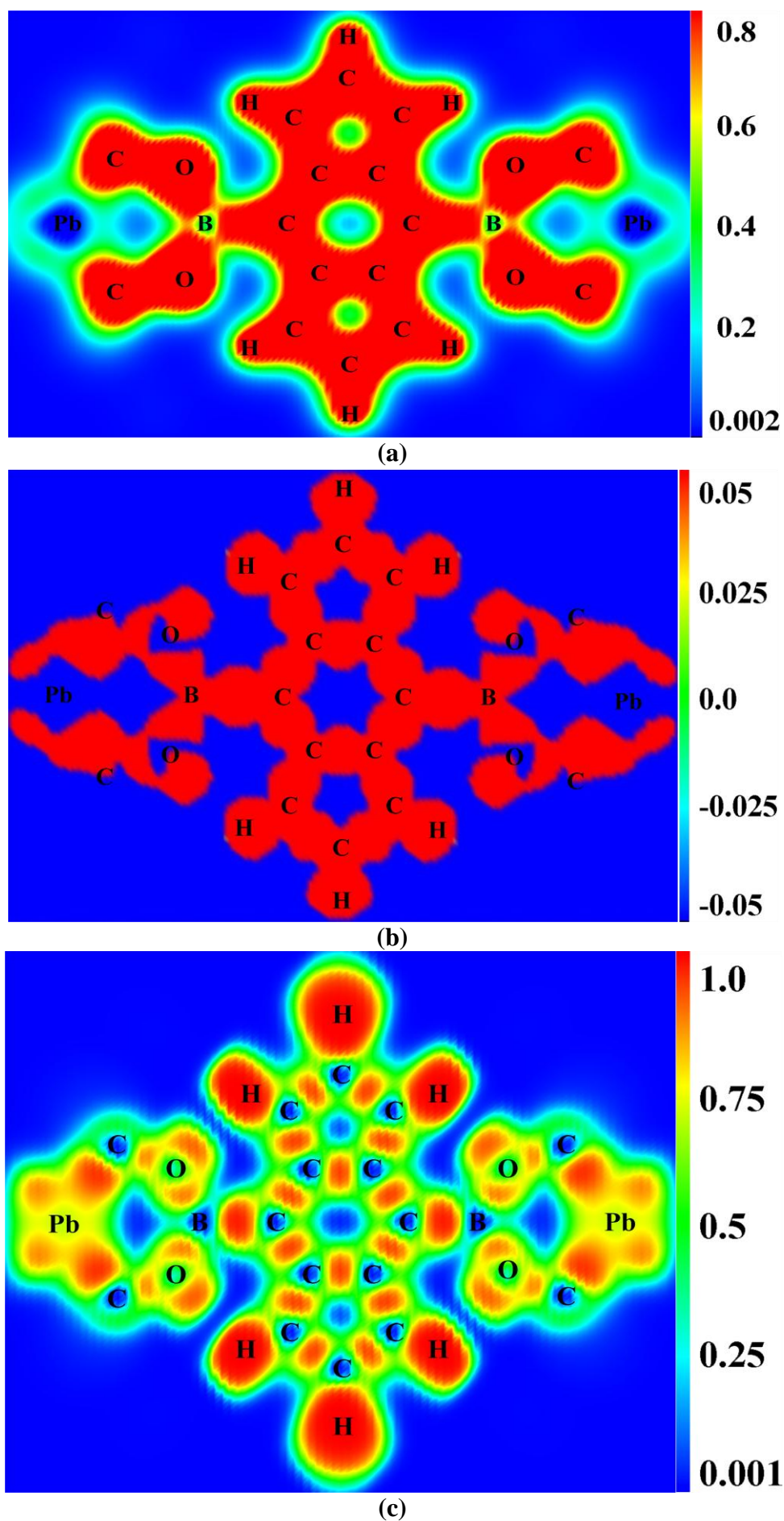
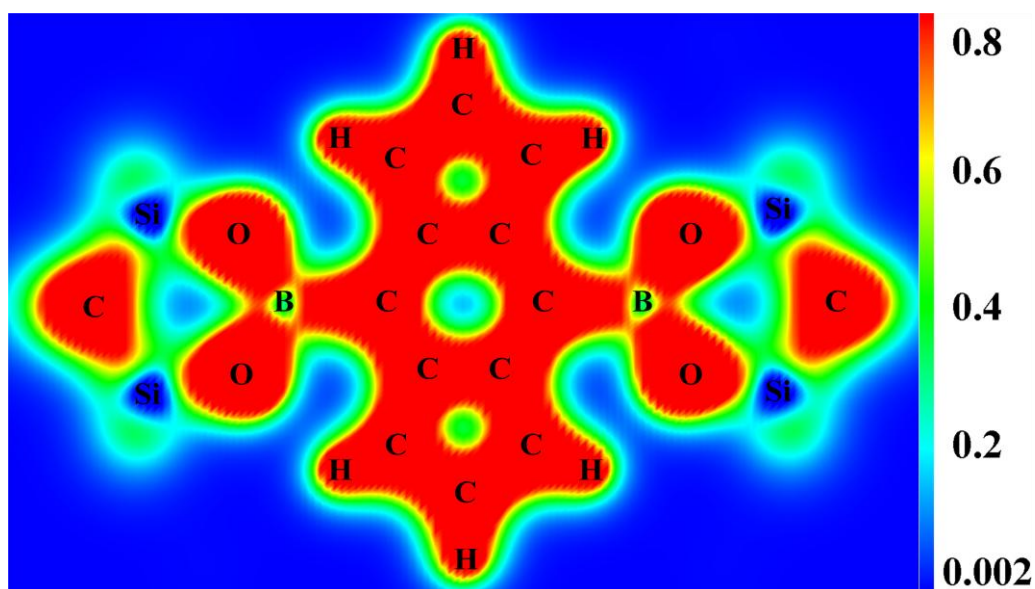
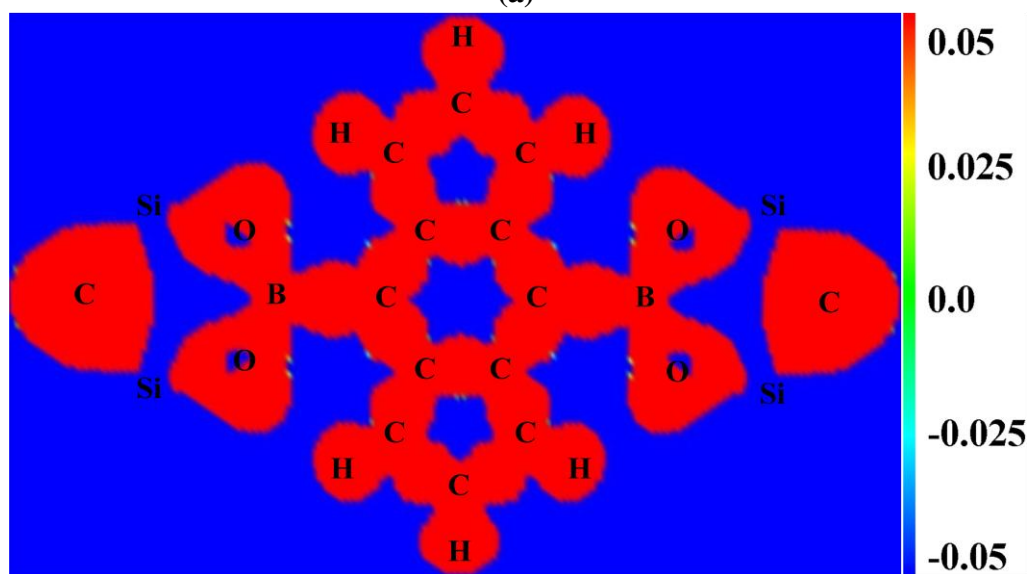


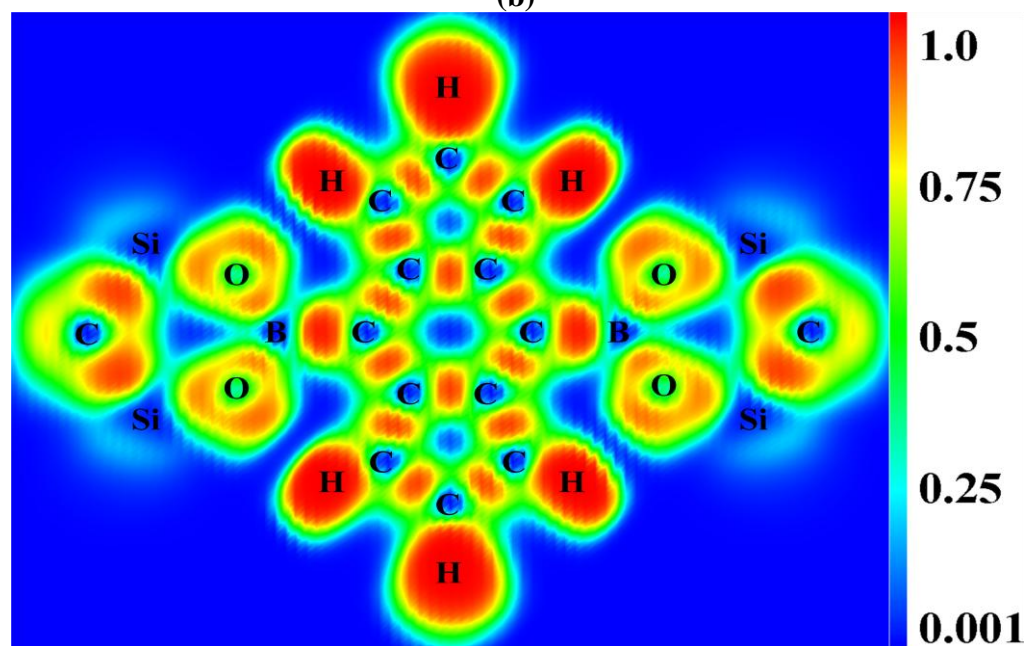
Figure S22. Calculated charge density (a) in $e\text{\AA}^3$, charge transfer (b) in $e\text{\AA}^3$, and electron localization function (c) plots for (C, Pb) in the (110) plane.



(a)



(b)



(c)

Figure S23. Calculated charge density (a) in $e/\text{\AA}^3$, charge transfer (b) in $e/\text{\AA}^3$, and electron localization function (c) plots for (Si, C) in the (110) plane.

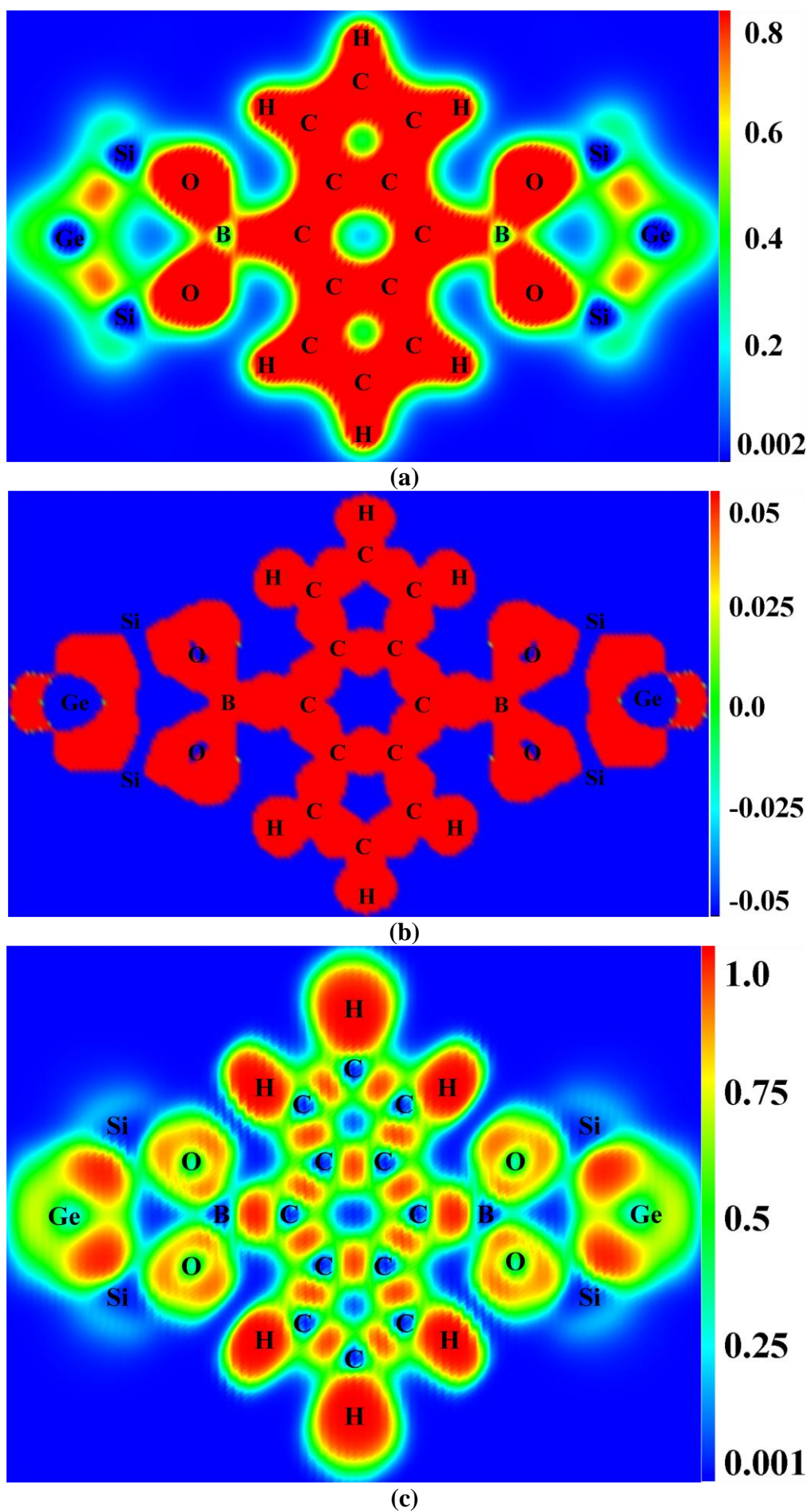
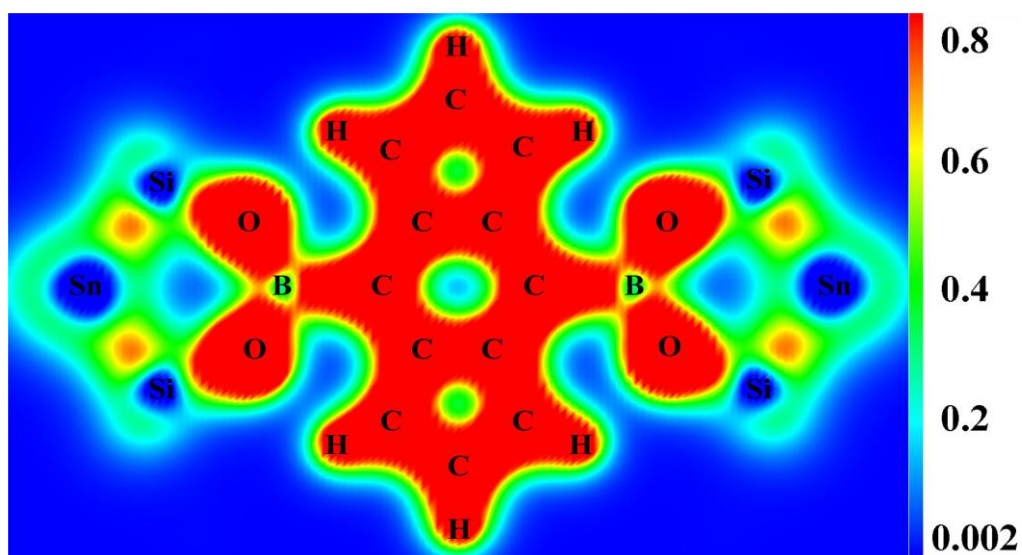
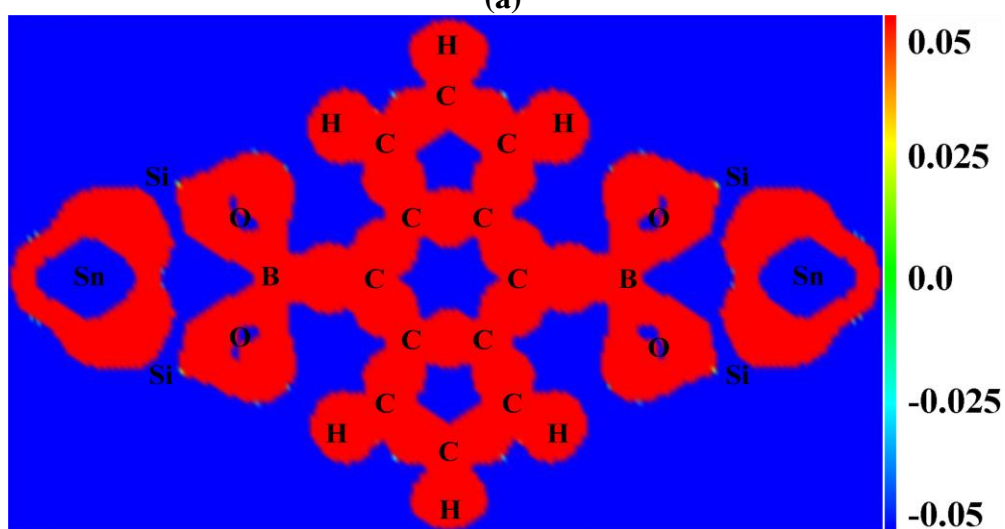


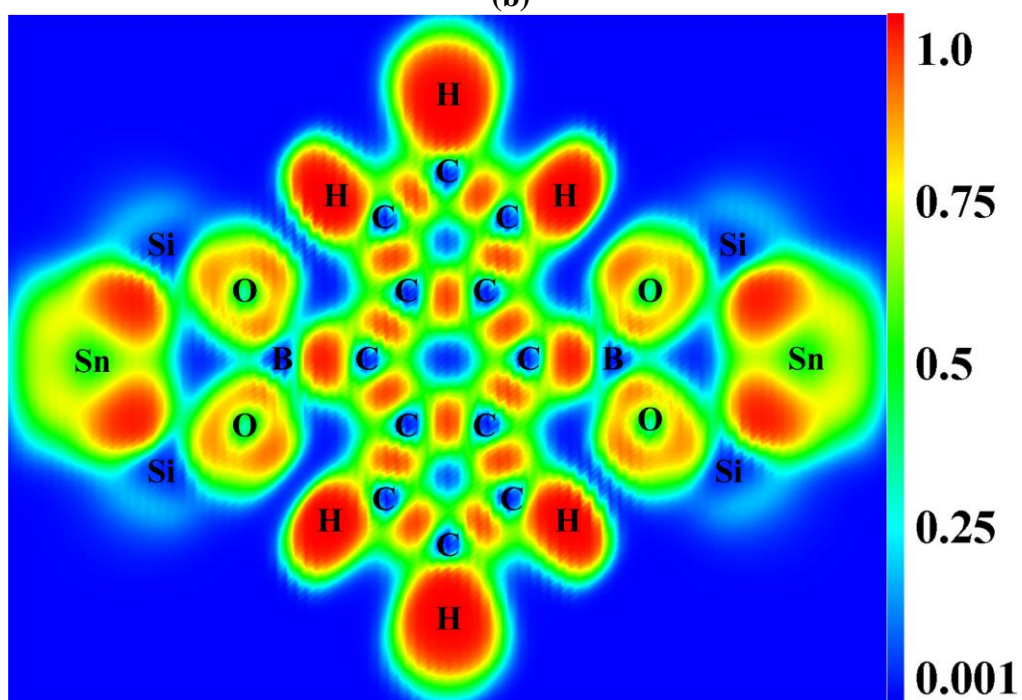
Figure S25. Calculated charge density (a) in $e/\text{\AA}^3$, charge transfer (b) in $e/\text{\AA}^3$, and electron localization function (c) plots for (Si, Ge) in the (110) plane.



(a)



(b)



(c)

Figure S26. Calculated charge density (a) in $e\text{\AA}^3$, charge transfer (b) in $e\text{\AA}^3$, and electron localization function (c) plots for (Si, Sn) in the (110) plane.

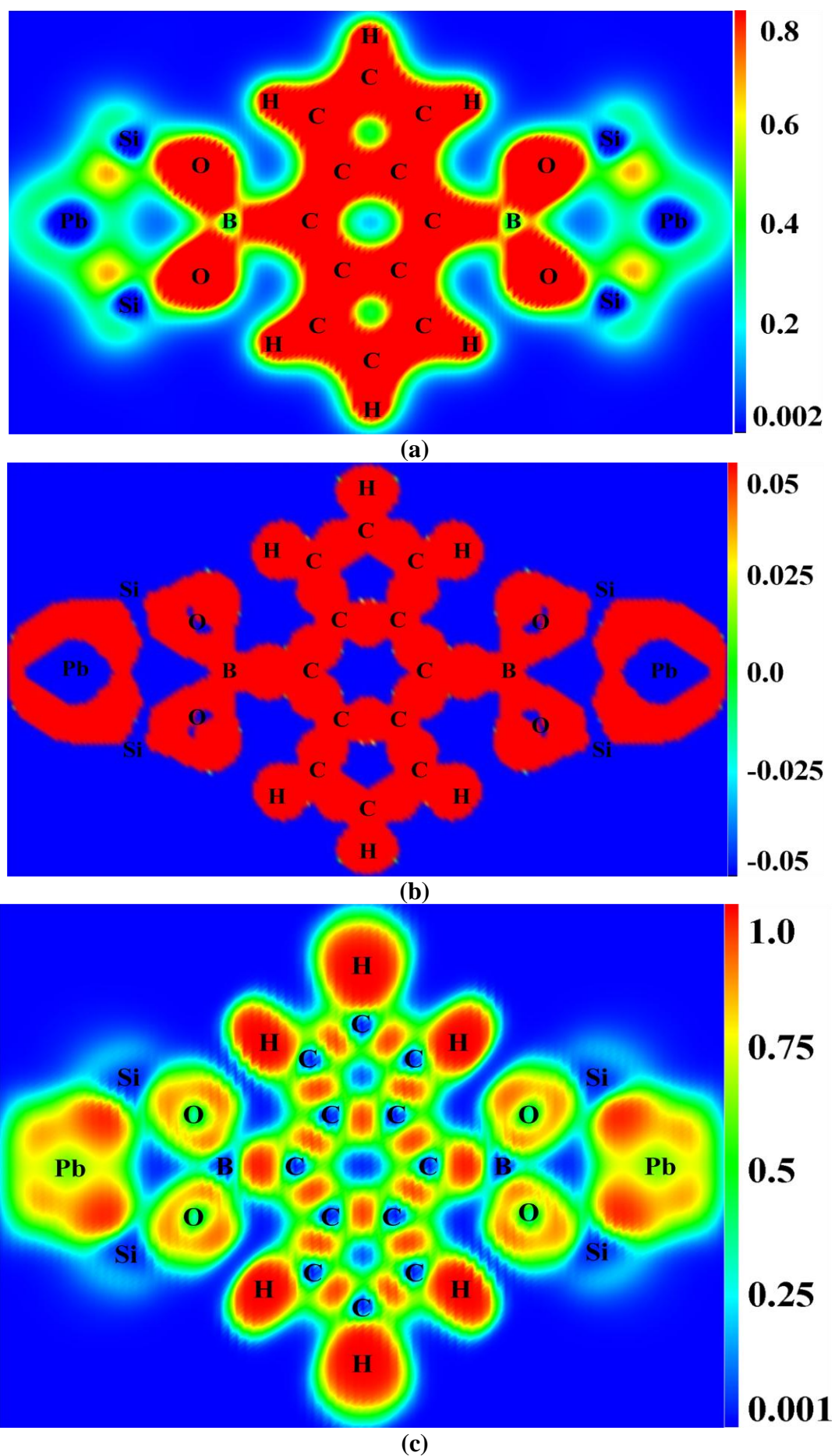


Figure S27. Calculated charge density (a) in $e/\text{\AA}^3$, charge transfer (b) in $e/\text{\AA}^3$, and electron localization function (c) plots for (Si, Pb) in the (110) plane.

Table S3. The calculated enthalpies of formation (ΔH ; $\text{kJ mol}^{-1}f.u.^{-1}$) according to eq 1 for the $[(X_4Y)(O_2B-C_{12}H_6-BO_2)_3]$ ($X=C/Si$; $Y=C, Si, Ge, Sn, \text{ and Pb}$) compounds. $1f.u.= [(X_4Y)(O_2B-C_{12}H_6-BO_2)_3]$

$(X_4Y)(O_2B-C_{12}H_6-BO_2)_3$	(C, C)	(C, Si)	(C, Ge)	(C, Sn)	(C, Pb)
$\Delta H (\text{kJ mol}^{-1}f.u.^{-1})$	-27.586	-27.88	-26.94	-22.90	-19.43
$(X_4Y)(O_2B-C_{12}H_6-BO_2)_3$	(Si, C)	(Si, Si)	(Si, Ge)	(Si, Sn)	(Si, Pb)
$\Delta H (\text{kJ mol}^{-1}f.u.^{-1})$	-51.55	-46.74	-46.895	-42.54	-40.08

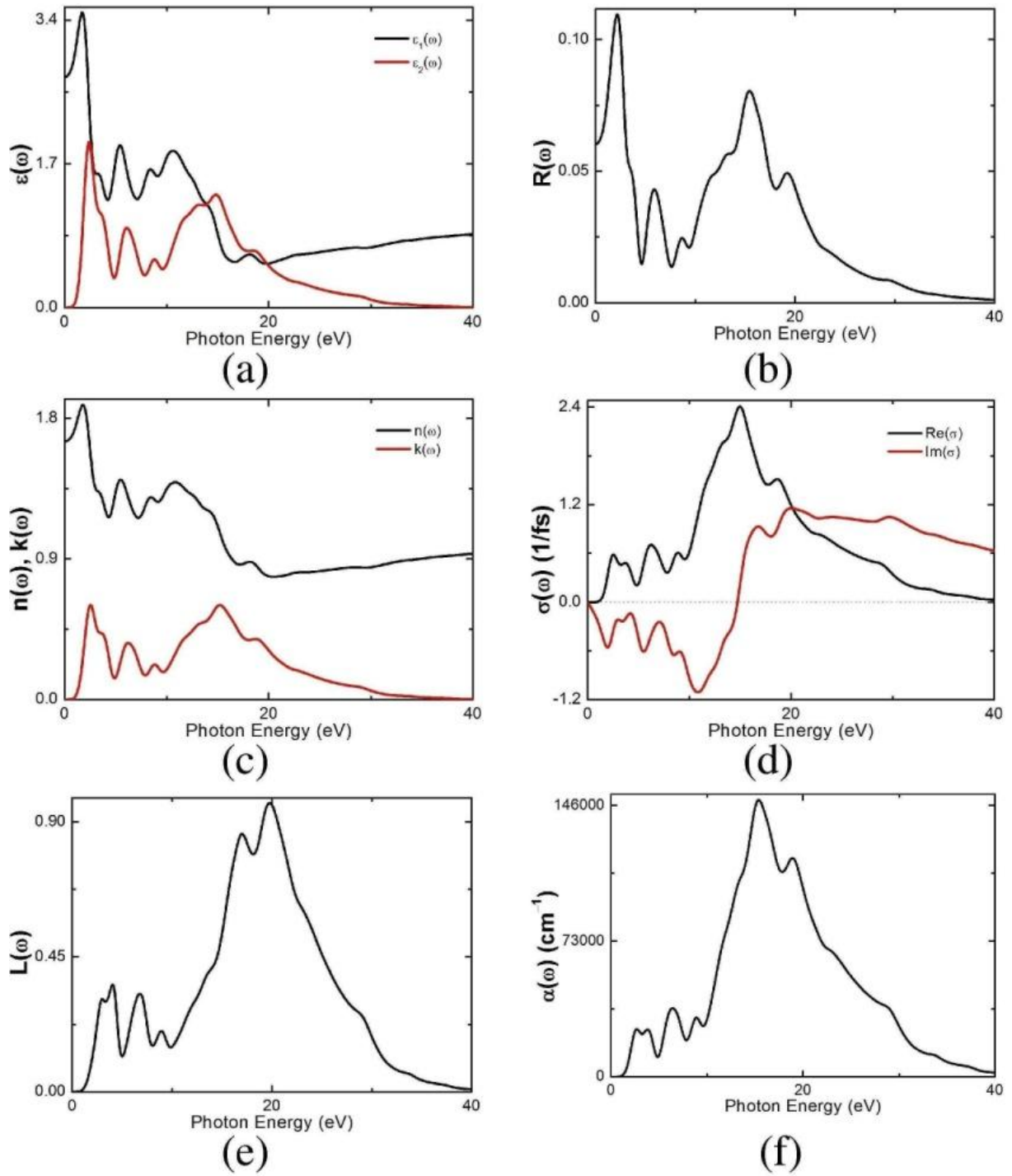


Figure S28. Calculated optical properties for (C, C): (a) dielectric function $\epsilon(\omega)$, (b) reflectivity $R(\omega)$, (c) refractive index $n(\omega)$; extinction coefficient $k(\omega)$, (d) optical conductivity $\sigma(\omega)$, (e) energy loss function $L(\omega)$, and (f) absorption $\alpha(\omega)$.

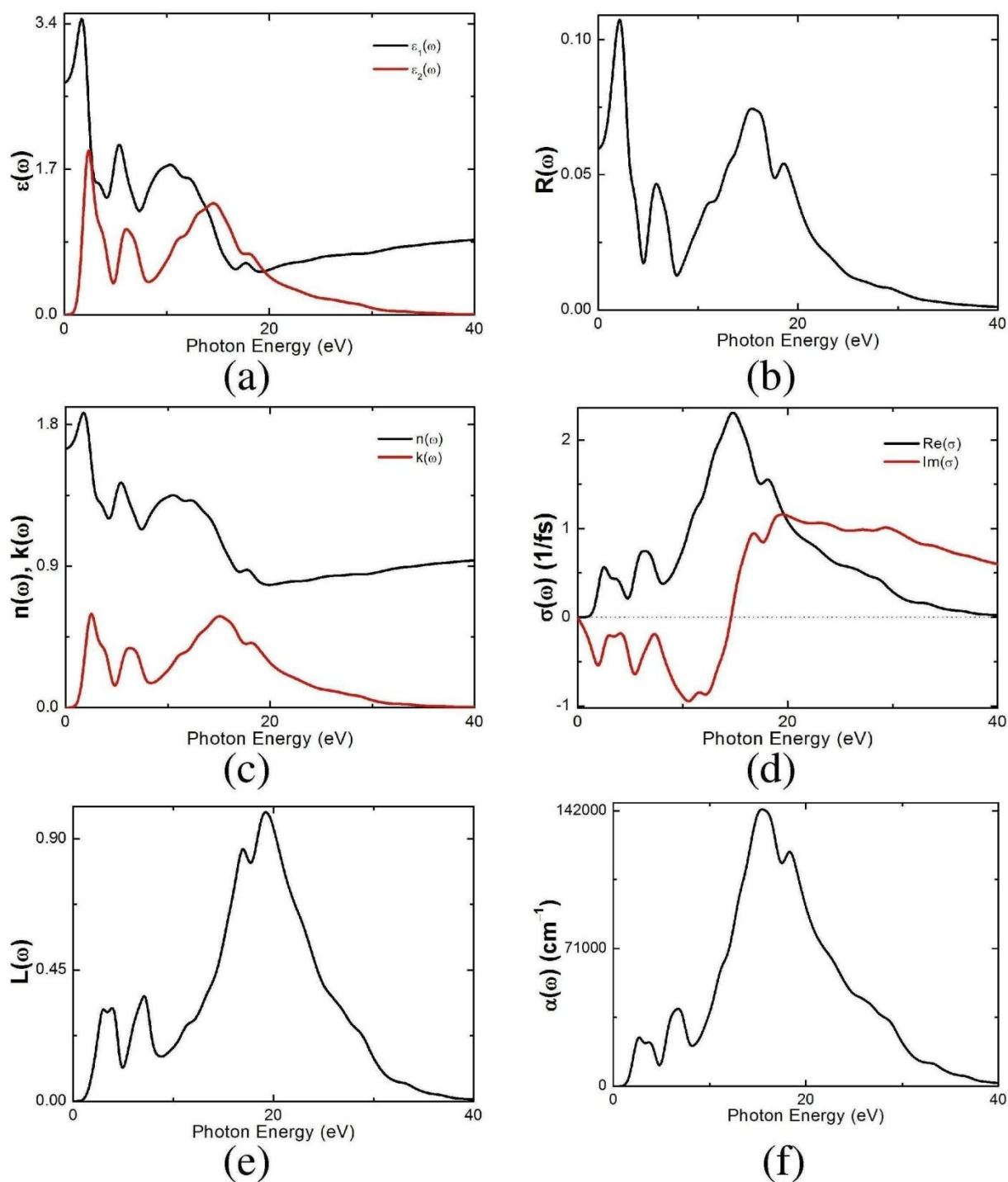


Figure S29. Calculated optical properties for (C, Si): (a) dielectric function $\epsilon(\omega)$, (b) reflectivity $R(\omega)$, (c) refractive index $n(\omega)$; extinction coefficient $k(\omega)$, (d) optical conductivity $\sigma(\omega)$, (e) energy loss function $L(\omega)$, and (f) absorption $\alpha(\omega)$.

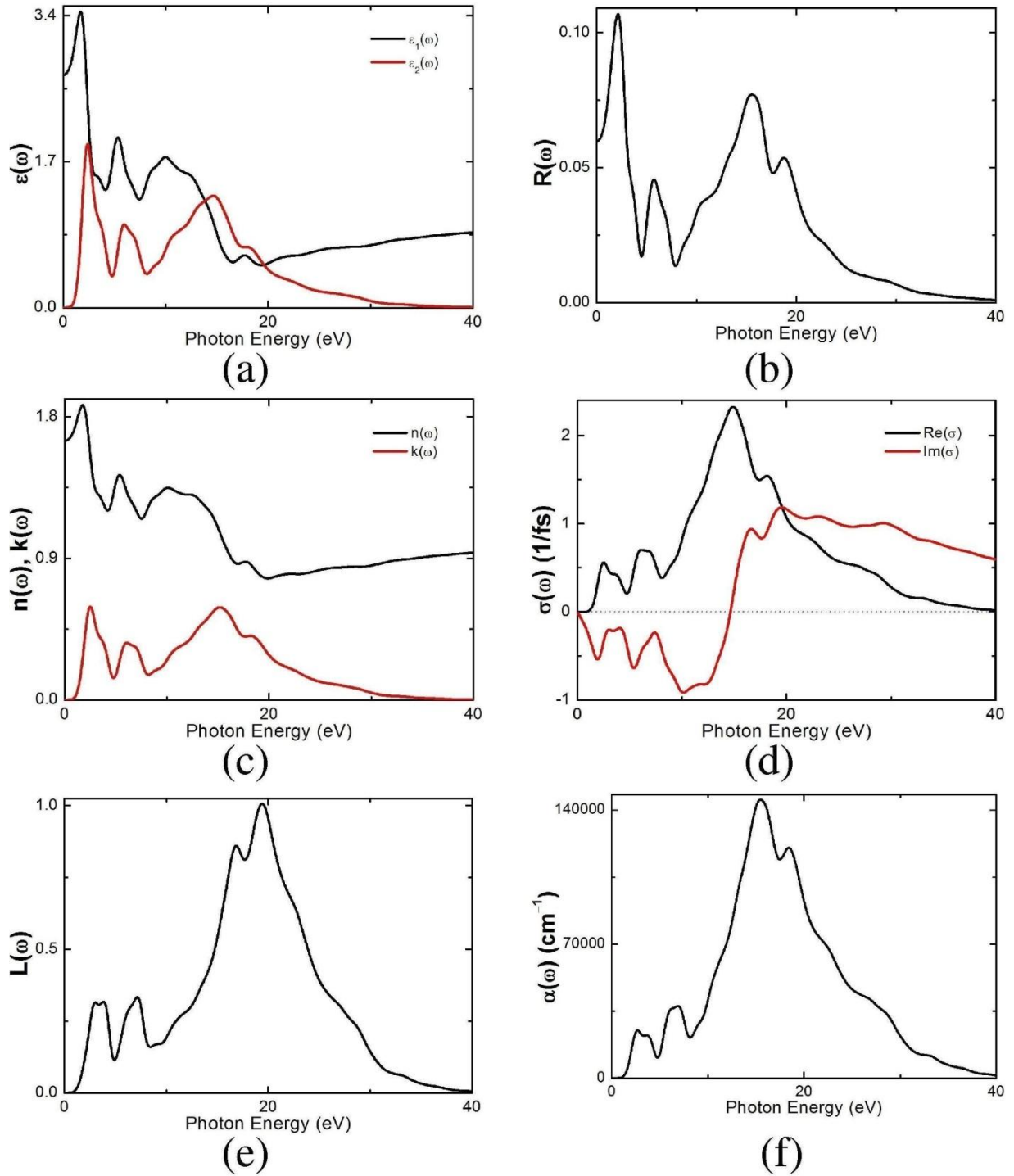


Figure S30. Calculated optical properties for (C, Ge): (a) dielectric function $\epsilon(\omega)$, (b) reflectivity $R(\omega)$, (c) refractive index $n(\omega)$; extinction coefficient $k(\omega)$, (d) optical conductivity $\sigma(\omega)$, (e) energy loss function $L(\omega)$, and (f) absorption $\alpha(\omega)$.

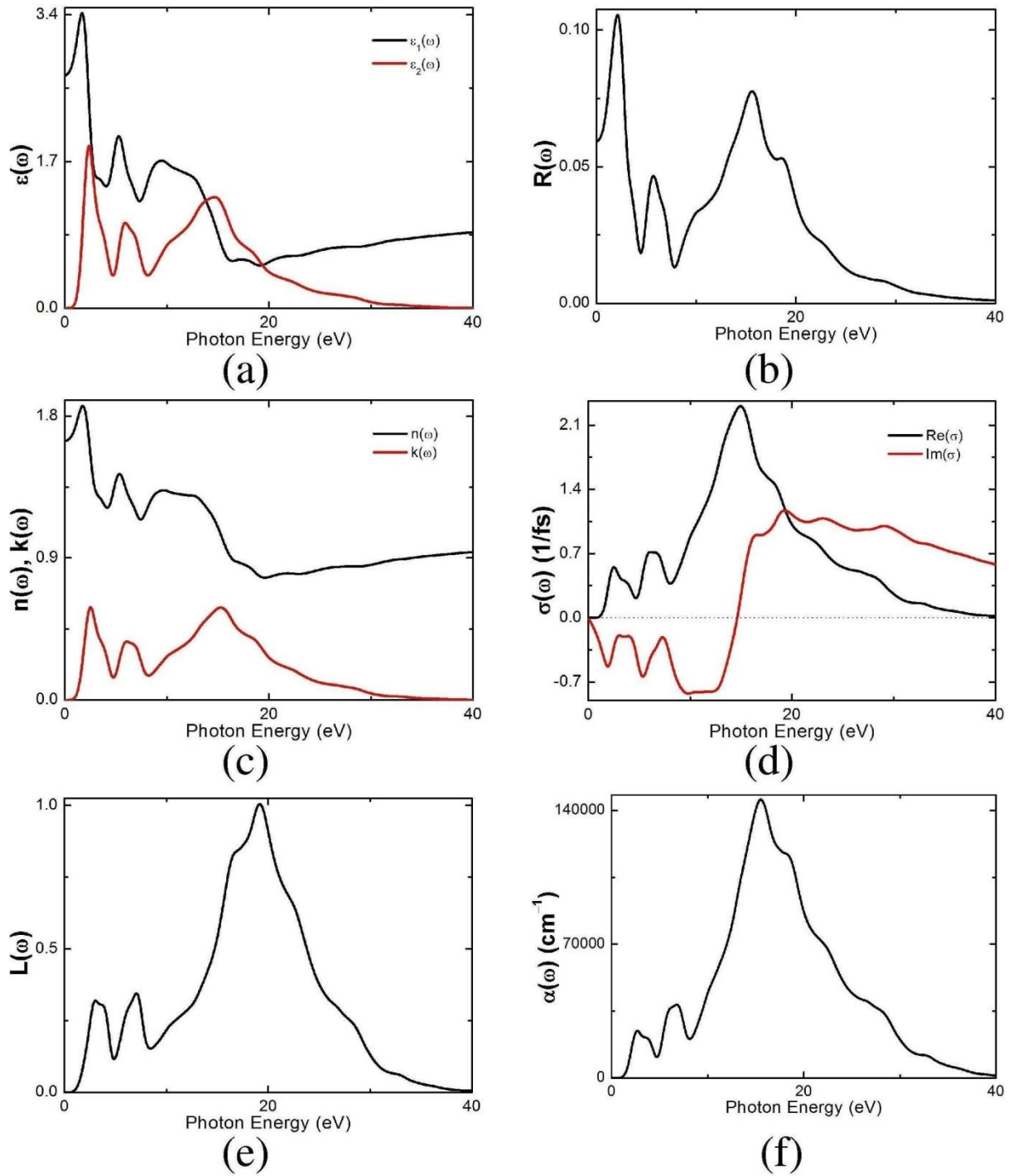


Figure S31. Calculated optical properties for (C, Sn): (a) dielectric function $\epsilon(\omega)$, (b) reflectivity $R(\omega)$, (c) refractive index $n(\omega)$; extinction coefficient $k(\omega)$, (d) optical conductivity $\sigma(\omega)$, (e) energy loss function $L(\omega)$, and (f) absorption $\alpha(\omega)$.

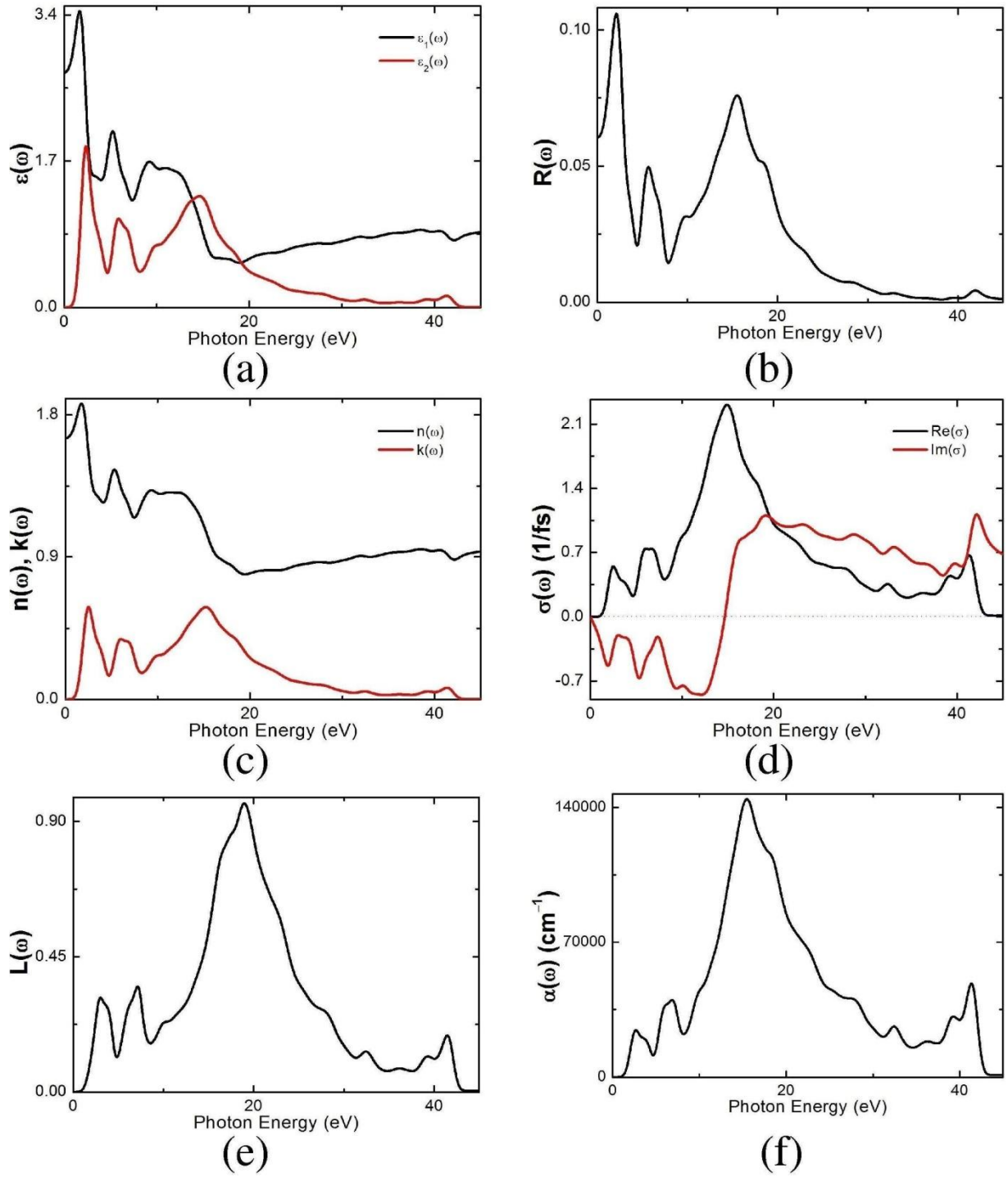


Figure S32. Calculated optical properties for (C, Pb): (a) dielectric function $\epsilon(\omega)$, (b) reflectivity $R(\omega)$, (c) refractive index $\mathbf{n}(\omega)$; extinction coefficient $\mathbf{k}(\omega)$, (d) optical conductivity $\sigma(\omega)$, (e) energy loss function $L(\omega)$, and (f) absorption $\alpha(\omega)$.

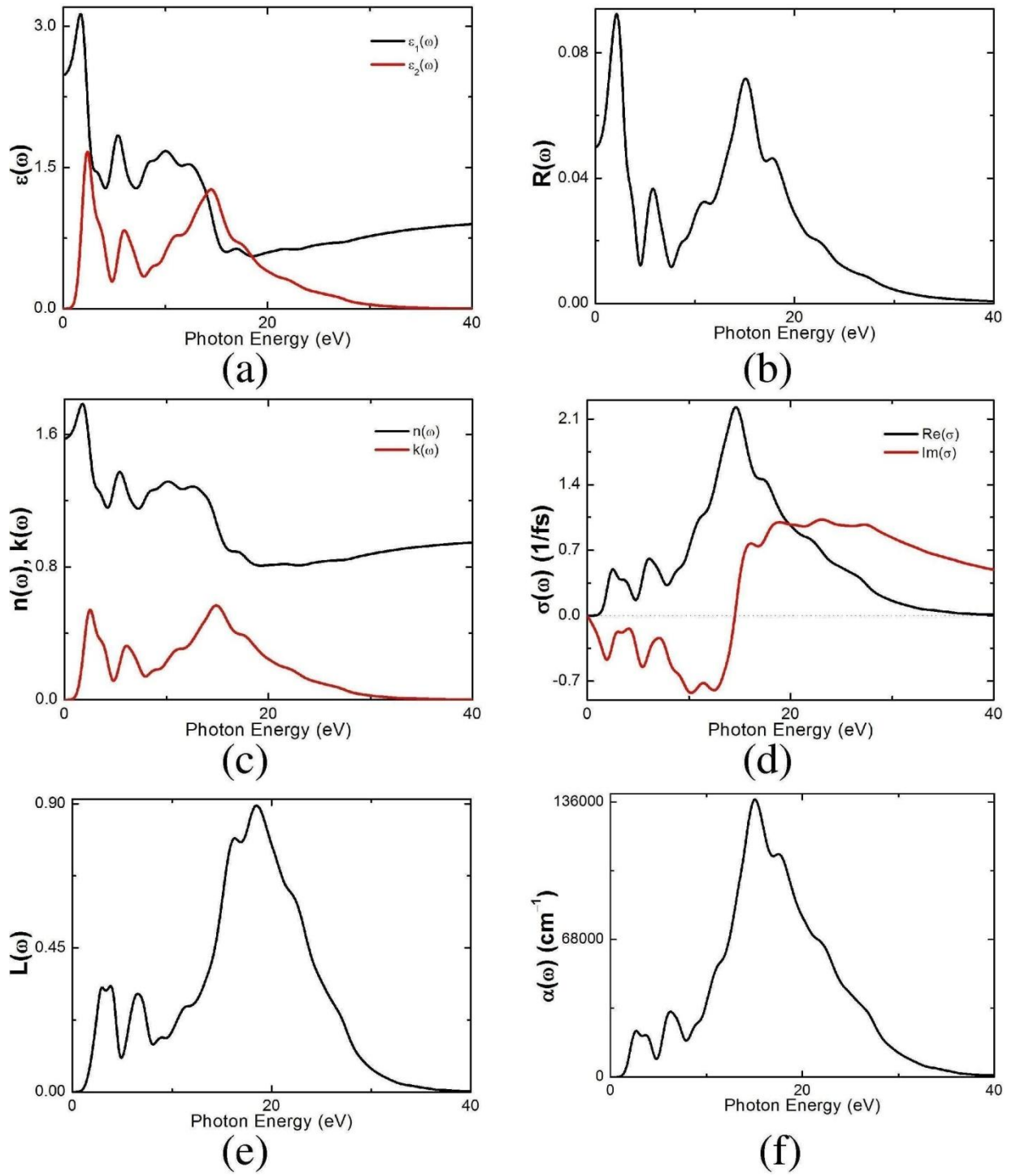


Figure S33. Calculated optical properties for (Si, C): (a) dielectric function $\epsilon(\omega)$, (b) reflectivity $R(\omega)$, (c) refractive index $n(\omega)$; extinction coefficient $k(\omega)$, (d) optical conductivity $\sigma(\omega)$, (e) energy loss function $L(\omega)$, and (f) absorption $\alpha(\omega)$.

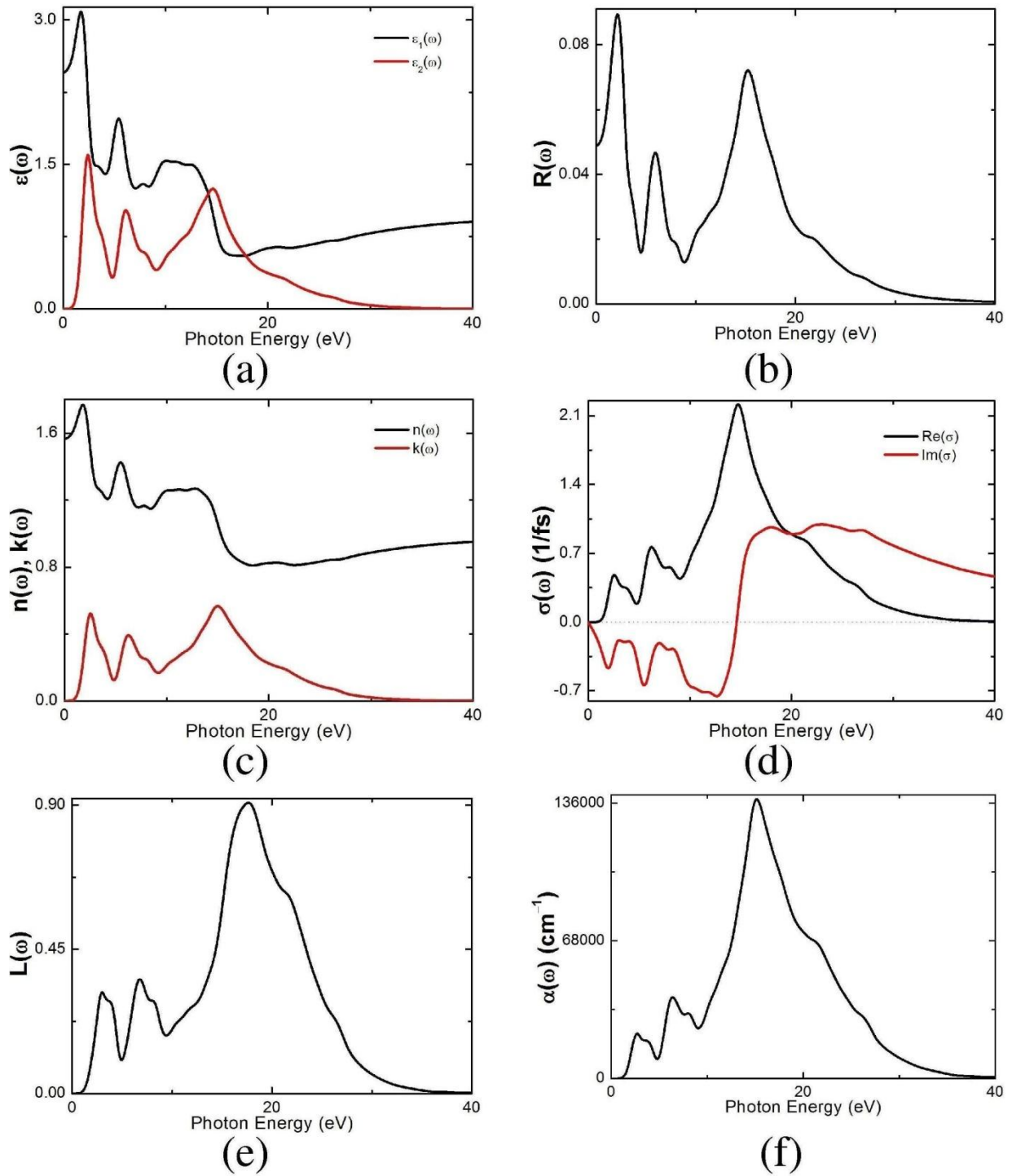


Figure S34. Calculated optical properties for (Si, Si): (a) dielectric function $\epsilon(\omega)$, (b) reflectivity $R(\omega)$, (c) refractive index $n(\omega)$; extinction coefficient $k(\omega)$, (d) optical conductivity $\sigma(\omega)$, (e) energy loss function $L(\omega)$, and (f) absorption $\alpha(\omega)$.

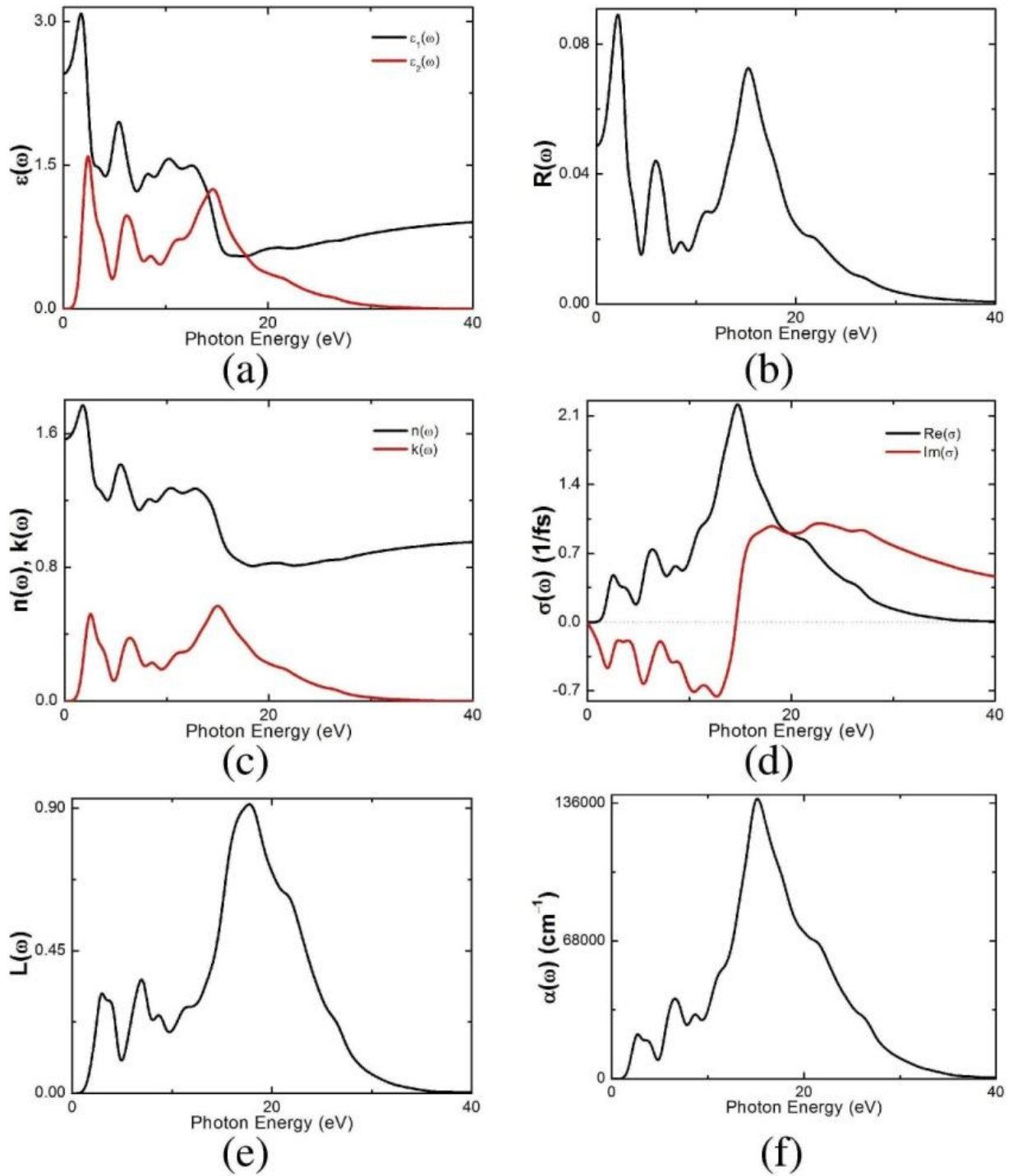


Figure S35. Calculated optical properties for (Si, Ge): (a) dielectric function $\epsilon(\omega)$, (b) reflectivity $R(\omega)$, (c) refractive index $n(\omega)$; extinction coefficient $k(\omega)$, (d) optical conductivity $\sigma(\omega)$, (e) energy loss function $L(\omega)$, and (f) absorption $\alpha(\omega)$.

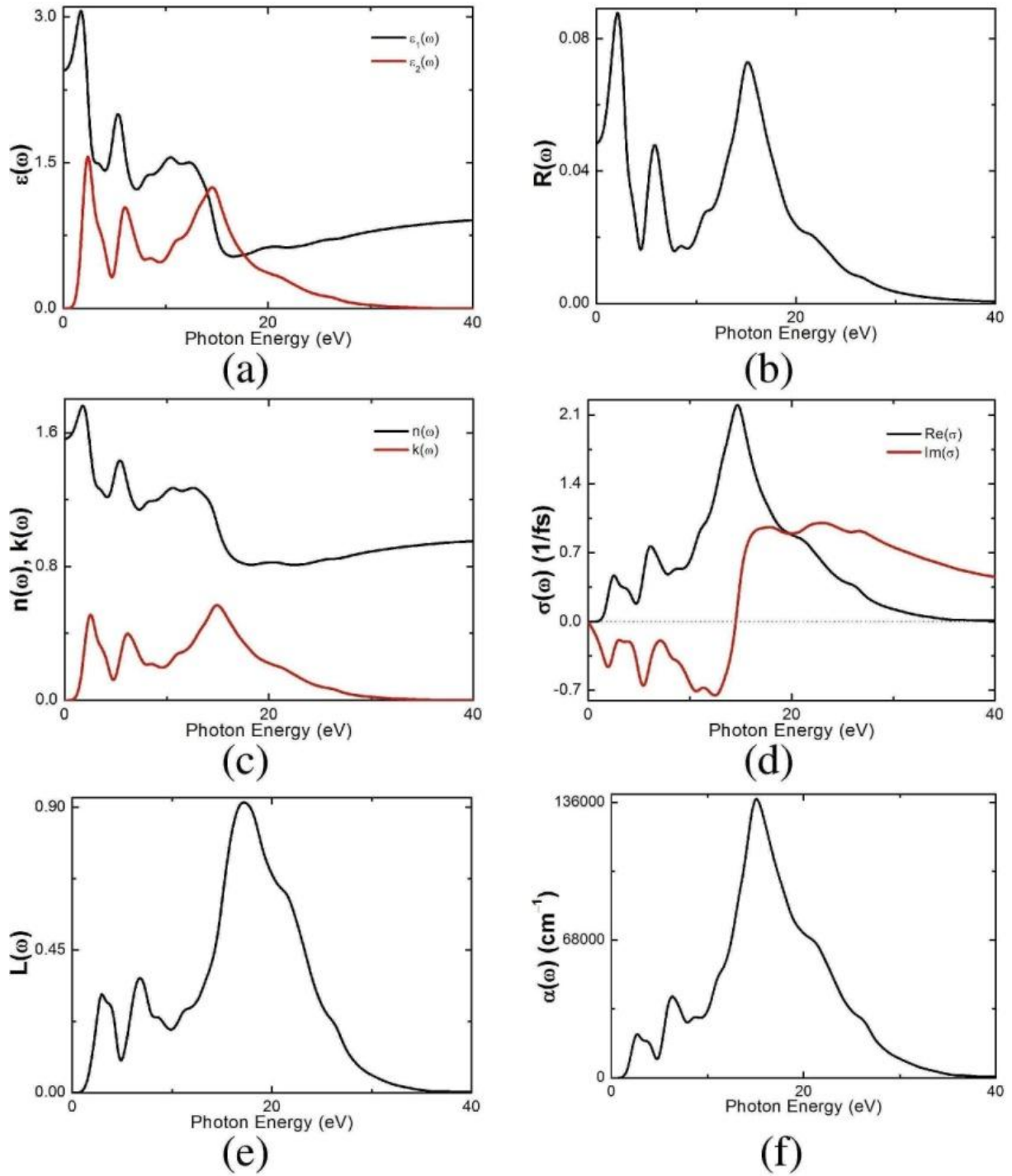


Figure S36. Calculated optical properties for (Si, Sn): (a) dielectric function $\epsilon(\omega)$, (b) reflectivity $R(\omega)$, (c) refractive index $n(\omega)$; extinction coefficient $k(\omega)$, (d) optical conductivity $\sigma(\omega)$, (e) energy loss function $L(\omega)$, and (f) absorption $\alpha(\omega)$.

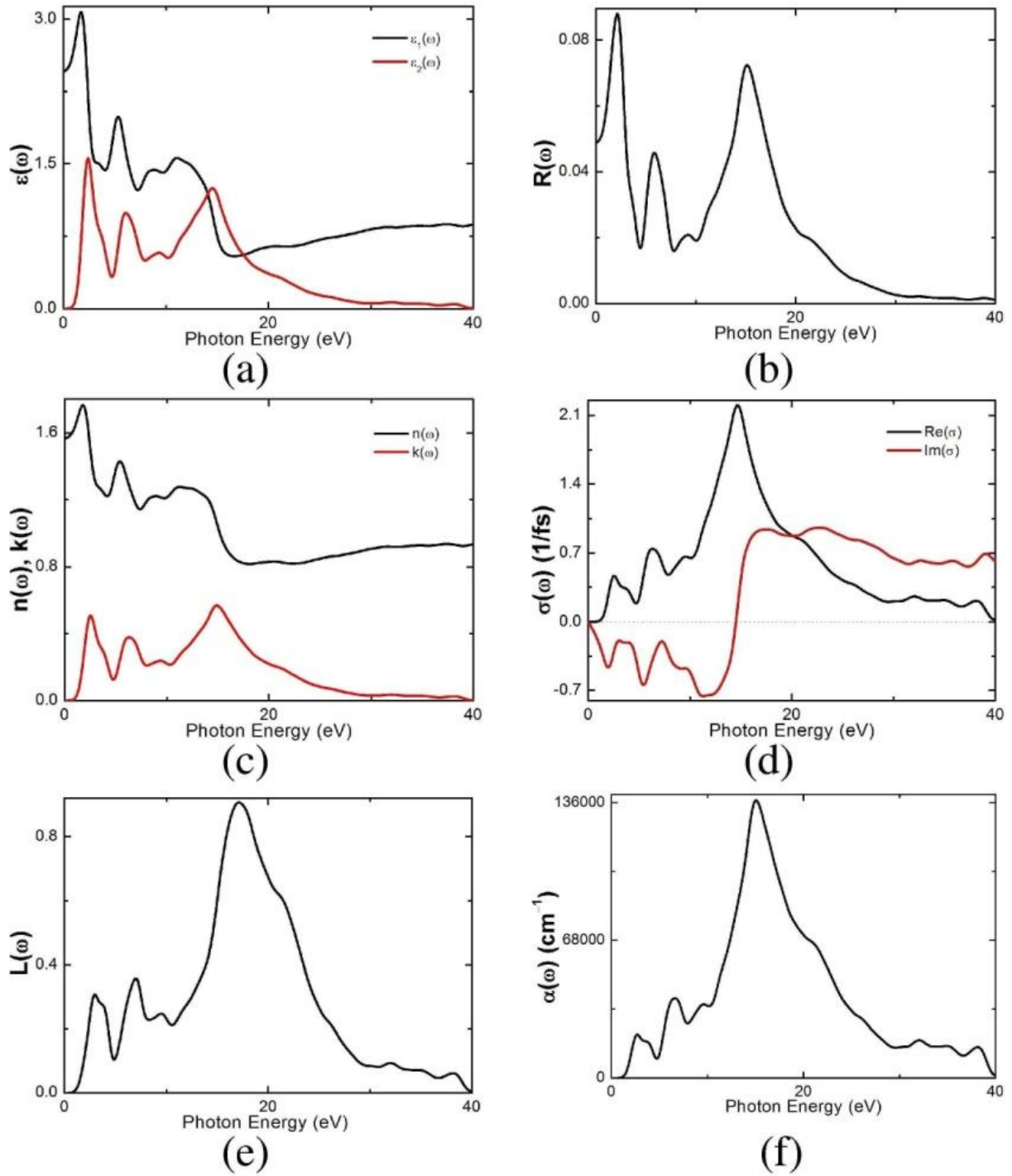


Figure S37. Calculated optical properties for (Si, Pb): (a) dielectric function $\epsilon(\omega)$, (b) reflectivity $R(\omega)$, (c) refractive index $n(\omega)$; extinction coefficient $k(\omega)$, (d) optical conductivity $\sigma(\omega)$, (e) energy loss function $L(\omega)$, and (f) absorption $\alpha(\omega)$.

Table S4. Optical constants at infinite wavelength or zero energy: $\varepsilon_1(0)$, $R(0)$, $n(0)$, and the maximum peaks of imaginary part of dielectric function $\varepsilon_2(\omega)$, extinction coefficient $k(\omega)$, the real part of optical conductivity $Re(\sigma)$, electron energy-loss function $L(\omega)$, absorption coefficient $\alpha(\omega)$ for the whole $[(X_4Y)(O_2B-C_{12}H_6-BO_2)_3]$ ($X=C/Si$; $Y=C-Pb$) series as well as that of MOF-5 for a comparison.

(X, Y)	(C, C)	(C, Si)	(C, Ge)	(C, Sn)	(C, Pb)	(Si, C)	(Si, Si)	(Si, Ge)	(Si, Sn)	(Si, Pb)	MOF-5
$\varepsilon_1(0)$	2.72308	2.7168	2.71297	2.70406	2.7329	2.48649	2.4559	2.4557	2.45057	2.4584	1.5286
$R(0)$	0.060373	0.059881	0.059881	0.059278	0.060598	0.049988	0.048926	0.048819	0.048555	0.048985	0.011244
$n(0)$	1.65017	1.64828	1.6471	1.6444	1.65315	1.57686	1.56714	1.56707	1.5654	1.5679	1.2364
$\varepsilon_2(\omega)$	1.95615	1.9137	1.9042	1.88017	1.8738	1.6675	1.59662	1.59154	1.5615	1.5569	0.8023
ω	2.3977	2.3805	2.37615	2.35304	2.3437	2.37079	2.41666	2.41595	2.39718	2.3922	15.0417
$k(\omega)$	0.60469	0.59518	0.5927	0.5879	0.5834	0.56839	0.56656	0.56797	0.5684	0.5675	0.3739
ω	2.55174	2.53184	2.52719	2.5026	2.5175	14.87597	15.0001	14.9957	14.9242	14.91587	15.2575
$Re(\sigma)$	2.40679	2.3073	2.3279	2.30487	2.31108	2.2289	2.21378	2.21375	2.20048	2.20225	1.4635
ω	14.97803	14.78799	14.88656	14.9656	14.9061	14.61885	14.74795	14.7207	14.6741	14.6663	15.1376
$L(\omega)$	0.96313	0.99048	1.00738	1.0052	0.96076	0.89498	0.9069	0.91166	0.9151	0.9061	0.6046
ω	19.7534	19.2264	19.3923	19.1781	18.9528	18.47558	17.65887	17.7453	17.1977	17.13928	16.4802
$\alpha(\omega)$	149054.6	142761.8	145341.2	145596.4	144318.6	137225.4	137814.8	138076.7	137578.5	137208.9	92324.8
ω	15.3888	15.46888	15.49069	15.51397	15.4771	15.06296	15.1605	15.15606	15.0833	15.0747	15.3774

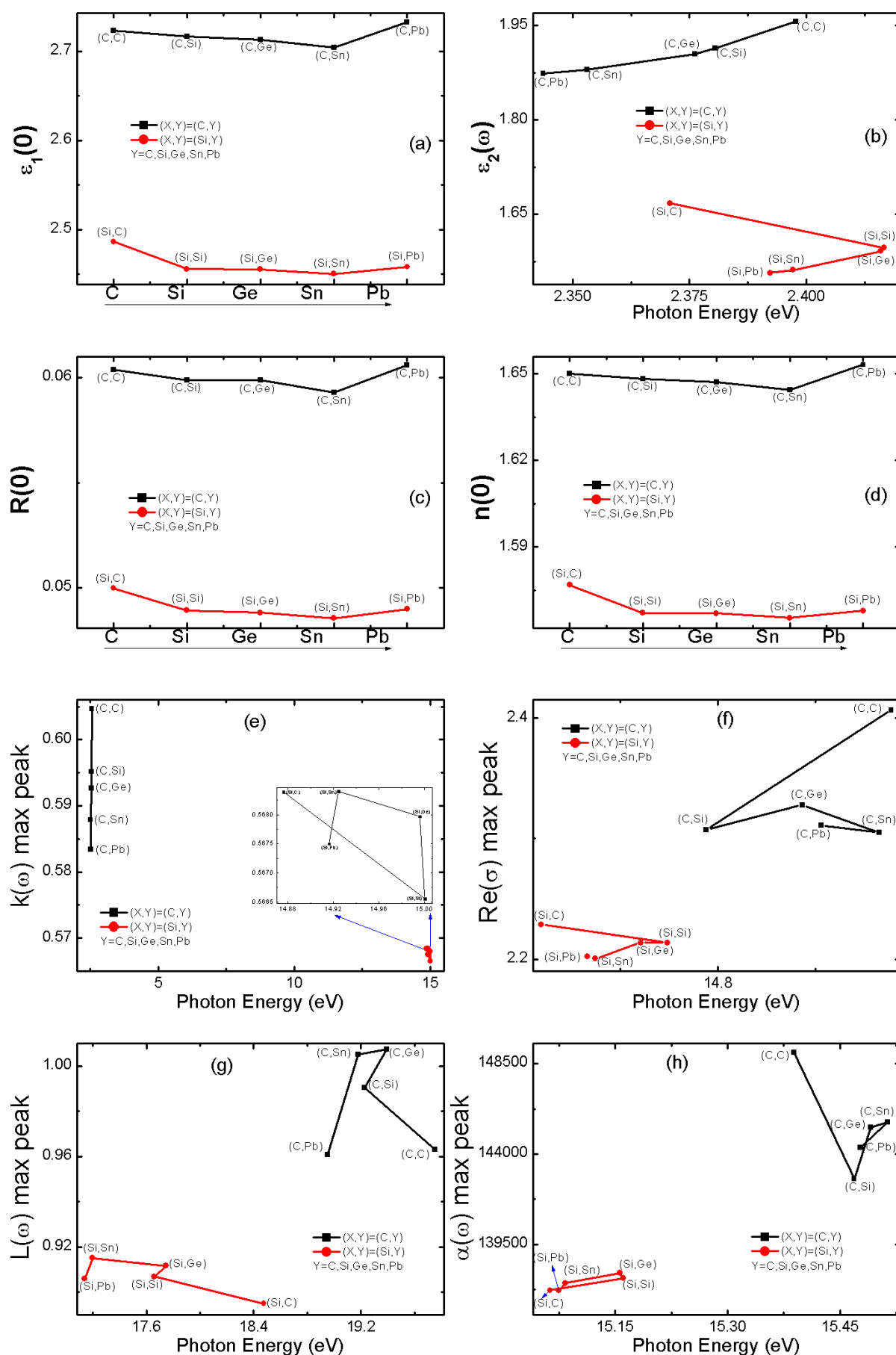


Figure S38. The special values of optical constants for the whole $(X_4Y)(O_2B-C_{12}H_6-BO_2)_3$, ($X=C/Si$; $Y=C-Pb$) series as well as that of MOF-5 for a comparison. we display the $\epsilon_1(0)$, $R(0)$, $n(0)$ in (a), (c), (d), respectively; the maximum peak of $\epsilon_2(\omega)$, $k(\omega)$, $Re(\sigma)$, $L(\omega)$, and $\alpha(\omega)$ in (b), (e), (f), (g), and (h), respectively.

References

- (1) Li, H.; Eddaoudi, M.; O'Keeffe, M.; Yaghi, O. M. *Nature* **1999**, *402*, 276.
- (2) Yang, L.-M.; Vajeeston, P.; Ravindran, P.; Fjellvag, H.; Tilset, M. *Inorg. Chem.* **2010**, *49*, 10283.
- (3) Yang, L.-M.; Fang, G.-Y.; Ma, J.; Ganz, E.; Han, S. S. *Cryst. Growth Des.* **2014**, *14*, 2532.
- (4) Alvaro, M.; Carbonell, E.; Ferrer, B.; Llabres i Xamena, F. X.; Garcia, H. *Chem. Eur. J.* **2007**, *13*, 5106.
- (5) Gascon, J.; Hernández-Alonso, M. D.; Almeida, A. R.; van Klink, G. P. M.; Kapteijn, F.; Mul, G. *ChemSusChem* **2008**, *1*, 981.
- (6) Bordiga, S.; Lamberti, C.; Ricchiardi, G.; Regli, L.; Bonino, F.; Damin, A.; Lillerud, K. P.; Bjorgen, M.; Zecchina, A. *Chem. Commun.* **2004**, 2300.